The IRM
Quarterly
Summer 2017, Vol. 27 No.2

ISSN: 2152-1972

Inside...

The New Deal- transitioning from a disordered to an ordered state

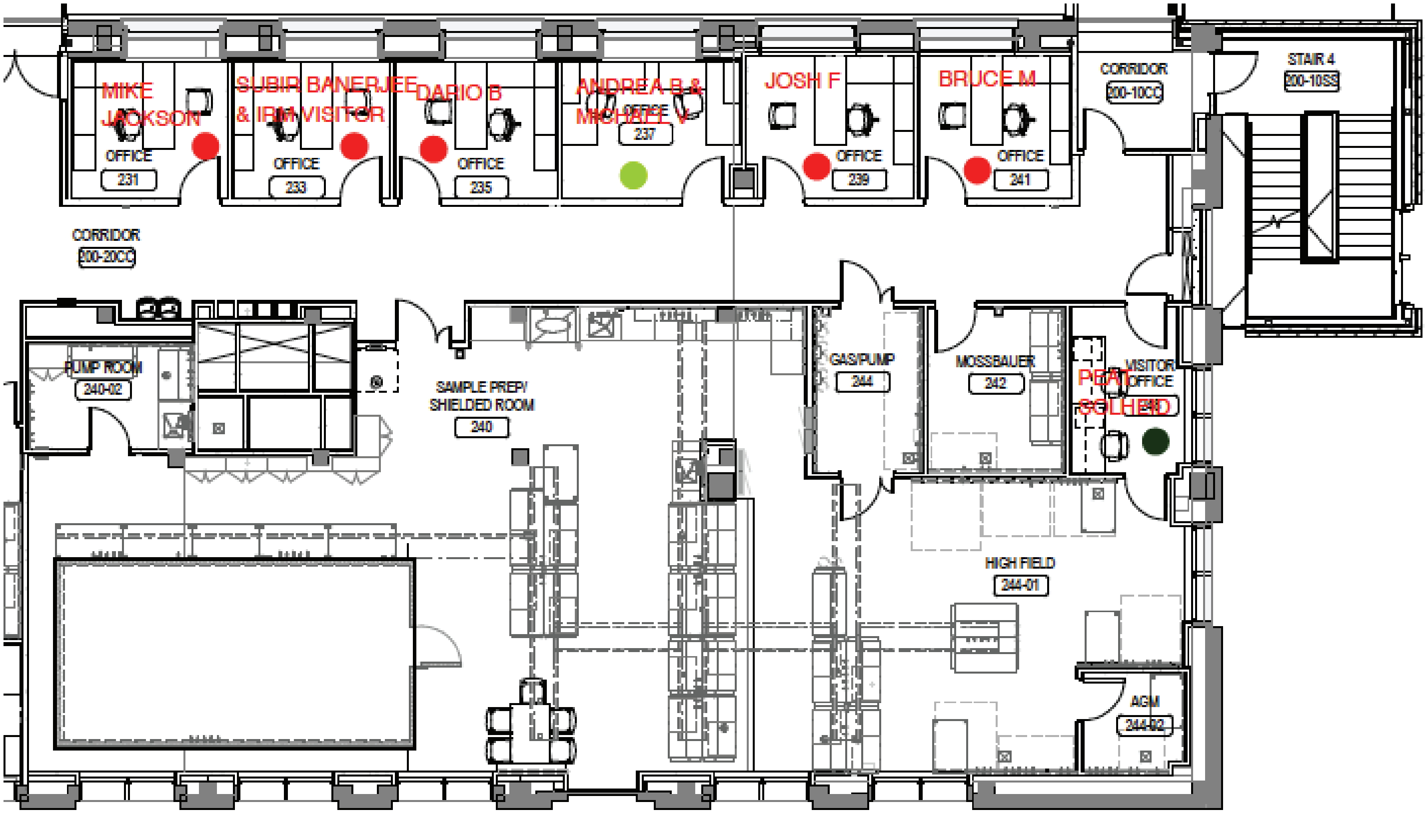

Fig. 1. Layout of the new Institute for Rock Magnetism. Plan is oriented with North at the top of the page. See text for details.

Dario Bilardello
Institute for Rock Magnetism
dario@umn.edu

The solar eclipse occurred on August 21st , and the sun set permanently on our home in Shepherd Labs. Almost five weeks have gone by since then, and in that time setting up the new space has gone, if not swiftly, at least without major complications.

The IRM *per se* is not yet "open for business" but the instruments are one by one being re-assembled and coming online, and undergoing testing and recalibration. The three susceptibility meters (KLY-2, MFK, Magnon) are now all working and the technician from Quantum Designs brought the MPMSs back to life last week.

Because more than a dozen Earth Science labs are being set up at the same time, it is understandably somewhat chaotic. Electricians and plumbers have been busy all through the building finalizing connections for various lab instruments; in the IRM that has included installing wall-mounted electrical transformers for the VSM electromagnets, and connecting cooling water lines to the rock-synthesis furnaces and to the helium compressors for the 2G magnetometers and the helium liquefier. The connections have finally all been made and passed inspection, allowing the final instrument set-ups: namely, initial cooling of the SRM and U-Channel magnetometers, and testing the VSMs.

We are hopeful that by the end of October everything will be fully functioning and we are confident that we'll be ready to host visitors in the new year. The largest feat, however, will probably be tidying up and finding a new (permanent) home for every item, making the lab REALLY functional. As I write, September 25th, surprises aside we should not require electricians or plumbers anymore, and only minor fixtures need installing around the lab by contractors.

So having said that, it is probably a good time to start showing the public what the new space actually looks like.

cont'd. on pg. 18...

Low Temperature AMS protocol using the MFK Kappabridge

Ran Issachar
Tel Aviv University, Israel
ranissachar@gmail.com

Measuring AMS at low temperature has the potential of characterizing the rock-magnetic fabric carried by paramagnetic minerals [Martin-Hernandez and Ferre, 2007]. Following to Curie-Weiss law, low temperature AMS (LT-AMS) enhances the effect of paramagnetic minerals because the volume susceptibility k increases as the temperature decreases (T) as $k= C/(T-\theta)$; where C is the specific mineral Curie constant and θ is the paramagnetic Curie temperature, which is zero for pure paramagnetic materials [e.g., Cullity, 1972]. Accordingly, at 77K (boiling temperature of liquid nitrogen) the paramagnetic susceptibility increases by a factor of ~3.8 relative to room temperature AMS at 295K. Diamagnetic susceptibility does not show temperature dependence [e.g. Cullity, 1972], whereas ferromagnetic minerals often show susceptibility changes at low temperatures, (e.g., Verwey transition in magnetite-titanomagnetite or Morin transition in hematite). Nevertheless, in rocks with low ferromagnetic components relative to the paramagnetic component, the paramagnetic minerals dominantly govern the susceptibility changes at low temperatures. Consequently, the measurements at LT-AMS amplify the contribution of the paramagnetic minerals in the rock specimen. Additionally, the LT measurements may help in separating the AMS into its paramagnetic, diamagnetic and ferromagnetic components [Martin-Hernandez and Ferre, 2007].

LT-AMS measurements are carried out by either measuring while the specimen is immersed in liquid nitrogen [e.g. Pares and van der Pluijm, 2002; Schmidt et al. 2007], or by cooling the specimen in liquid nitrogen prior to measuring in air [e.g. Lüneburg et al., 1999; Oliva-Urcia et al. 2010]. The former has the advantage of keeping the specimen at homogeneous and constant temperature but requires a custom-made holder, which is not suitable for most susceptibility meters. For the latter, the measurement procedure is much simpler but an increase in temperature during the measurement is inevitable, together with other complications involving instrument failures. Many studies [Cifelli et al., 2004, 2005, 2009, 2011; Debacker et al., 2009; Oliva-Urcia et al., 2012, 2013, 2011; Soto et al., 2012, 2014; Garcia-Lasanta et al., 2013; Haerinck et al., 2013; Izquierdo-Llavall et al., 2013; García-Lasanta et al., 2014; Santolaria et al., 2015] followed Lüneburg et al.'s [1999] and Oliva-Urcia et al.'s [2010] protocols, characterizing the LT-AMS of rocks, mainly due to the standardization of the equipment used and the popularity of the Agico Kappabridge susceptibility meter.

We propose a protocol to measure the LT-AMS in air using the Agico Kappabridge with the spinning specimen holder, which allows fast and consistent measurements. The protocol tackles two main instrumental obstacles, which are caused by the low temperature of the specimen and leads to significant measurement errors or even failure:

1. Operation of the spinning specimen holder. In the slowly spinning specimen method, the directional susceptibilities are measured for 5 or 8 revolutions as the specimen rotates around three perpendicular axis [Jelinek, 1995; Gee et al., 2008]. Susceptibilities are recorded in 64 positions per revolution and averaged for all revolutions [Gee et al., 2008]. The measurement is completed with an addition of one bulk susceptibility measurement. The spinning specimen method is faster and more accurate than the manual 15 positions method. Nevertheless, while introducing the cold specimen, the holder mechanically underperforms as friction is increasing. This can cause increased measurement errors or even failure.

2. Instrument drift. The cold sample, which is placed in the coil, leads to cold air convection and drift of the electrical components. This leads to significant errors and halt of measurements for an hour or more.
The proposed protocol is detailed as follows:

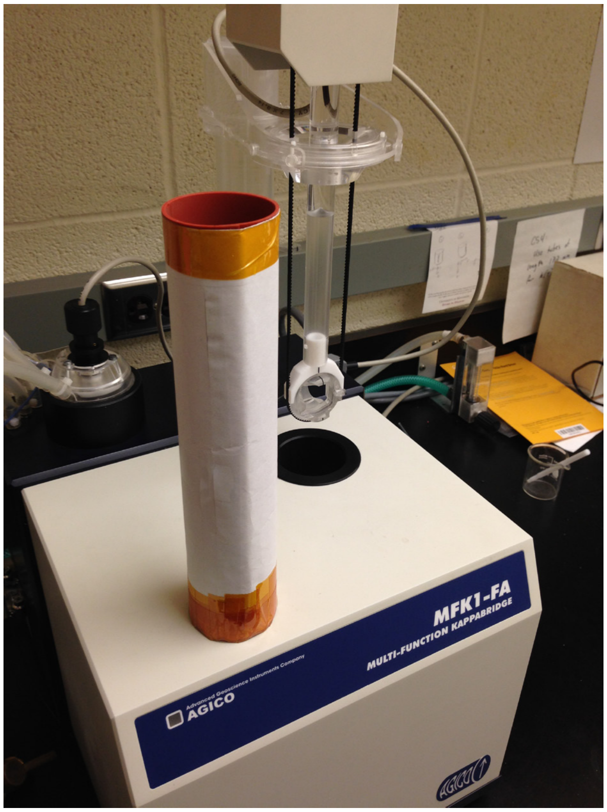

Fig. 1. Silicone sleeve to be inserted in the sample cavity of the susceptibility bridge.

Preparing the instrument

- Prepare a silicone sleeve using a silicon sheet, widely available in kitchen supply stores, that is ~3mm thick. Seal the sleeve using Kapton tape, also closing off the bottom of the cylinder (see Fig. 1.). The sleeve plus tape outer diameter will fit snugly inside the kappabridge bore.

- Immerse the samples in liquid nitrogen for about 50 minutes.
- Insert silicone sleeve inside the kappabridge, if not done so already.
- Put thin Teflon wire on the left side of the holder (see Fig. 2.) to prevent this from rapid cooling when sample is fixed.
- Turn on the kappabridge, following the AGICO start up procedure with the rotator enabled.
- Run the holder correction (repeat if bad).
- Move the holder counterclockwise, run empty axial measurement and spray gently TFL-50 (or other Teflon based lubricant) in the two points (see Fig. 3.) while the holder is rotating, to lubricate the holder.
- Run at least three more empty axial measurement runs so the lubricant will distribute itself evenly between the rotating sample holder and the white plastic bracket above

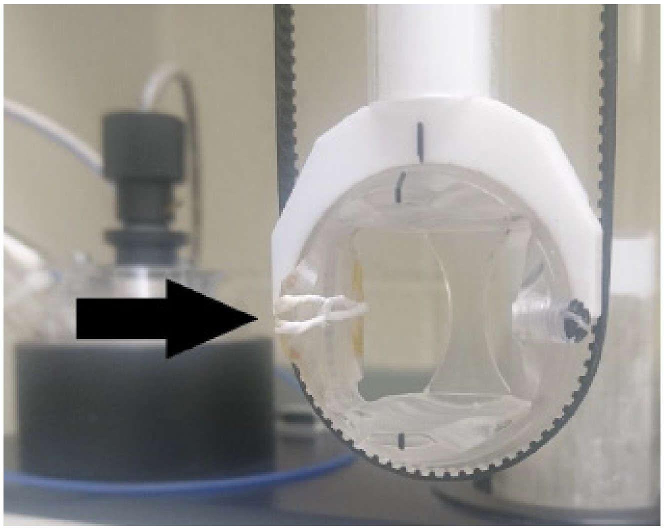
Fig.2. Teflon wire on holder.

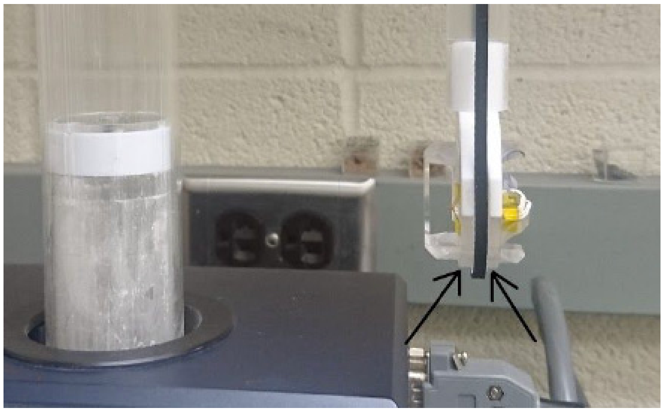
Fig. 3. points on the sample holder to be lubricated.

Measuring the samples

- Place a small sheet of paper over the kappabridge's sample cavity to prevent condensed air from entering the coil while fixing the sample in the holder.
- Take a sample out of liquid nitrogen and quickly place it in the holder.
- Remove the paper and run first axial measurement.
- After measurement, quickly place the sample back into liquid nitrogen.
- Wait at least 5 minutes to allow the instrument to stabilize and the sample to cool.
- Measure the second and third axial measurements as above.
- For the bulk susceptibility measurement, remove the sheet of paper as the holder goes down and replace it as the holder comes up.

Errors

- If the CHECKING ROTATOR PERIOD message appears at the end of an axial measurement for longer than two seconds, then the rotator need lubricating.
- If the instrument fails ZEROING, then the coil is too cold and needs to equilibrate longer.

References

Cifelli, F., M. Mattei, A. M. Hirt, and A. Gunther (2004), The origin of tectonic fabrics in "undeformed" clays: The early stages of deformation in extensional sedimentary basins, Geophys. Res. Lett., 31, L09604, doi:10.1029/2004GL019609.

Cifelli, F., M. Mattei, and M. Chadima (2005), The origin of tectonic lineation in extensional basins: combined neutron texture and magnetic analyses on "undeformed" clays, Earth Planet. Sci. Lett., 235(1), 62–78.

Cifelli, F., M. Mattei, M. Chadima, S. Lenser, and A. M. Hirt (2009), The magnetic fabric in "undeformed clays": AMS and neutron texture analyses from the Rif Chain (Morocco), Tectonophysics, 466(1-2), 79–88, doi:10.1016/j.tecto.2008.08.008.

Cifelli, F., L. Minelli, F. Rossetti, G. Urru, and M. Mattei (2011), The emplacement of the Late Miocene Monte Capanne intrusion (Elba Island, Central Italy): constraints from magnetic fabric analyses, Int. J. Earth Sci., 101(3), 787–802, doi:10.1007/s00531-011-0701-z.

Cullity, B. D. (1972), Introduction to Magnetic Materials, John Wiley & Sons, Hoboken, N. J.

Garcıa-Lasanta, C., B. Oliva-Urcia, T. Roman-Berdiel, A. M. Casas, and A. M. Hirt (2014), Understanding the Mesozoic kinematic evolution in the Cameros basin (Iberian Range, NE Spain) from magnetic subfabrics and mesostructures, J. Struct. Geol., 66, 84–101, doi:10.1016/j.jsg.2014.05.013.

Gee, J. S., L. Tauxe, and C. Constable (2008), AMS-Spin: A LabVIEW program for measuring the anisotropy of magnetic susceptibility with the Kappabridge KLY-4S, Geochem., Geophys. Geosyst., 9, Q08Y02, doi:10.1029/2008GC001976.

Jelinek, V. (1995), Measuring anisotropy of magnetic susceptibility on a slowly spinning specimen-basic theory, AGICO Print 10.

Luneburg, C. M., S. A. Lampert, H. D. Lebit, A. M. Hirt, M. Casey, and W. Lowrie (1999), Magnetic anisotropy, rock fabrics and finite strain in deformed sediments of SW Sardinia (Italy), Tectonophysics, 307(1-2), 51–74, doi:10.1016/S0040-1951(99)00118-3.

Martin-Hernandez, F., and E. C. Ferre (2007), Separation of paramagnetic and ferrimagnetic anisotropies: A review, J. Geophys. Res., 112, B03105, doi:10.1029/2006JB004340.

Oliva-Urcia, B., J. Rahl, A. Schleicher, and J. Pares (2010), Correlation between the anisotropy of the magnetic susceptibility, strain and X-ray Texture Goniometry in phyllites from Crete, Greece, Tectonophysics, 486(1), 120–131.

Pares, J. M., and B. A. van der Pluijm (2002), Phyllosilicate fabric characterization by Low-Temperature Anisotropy of

Magnetic Susceptibility (LT-AMS), Geophys. Res. Lett., 29(24), 2215, doi:10.1029/2002GL015459.

Santolaria, P., A. M. Casas, and R. Soto (2015), Anisotropy of magnetic susceptibility as a proxy to assess internal deformation in diapirs: case study of the Naval salt wall (Southern Pyrenees), Geophys. J. Int., 202(2), 1207–1222, doi:10.1093/gji/ggv231.

Schmidt, V., A. M. Hirt, P. Rosselli, and F. Martin-Hernandez (2007), Separation of diamagnetic and paramagnetic anisotropy by high-field, low-temperature torque measurements, Geophys. J. Int., 168(1), 40–47, doi:10.1111/j.1365-246X.2006.03202.x.

Soto, R., J. C. Kullberg, B. Oliva-Urcia, A. M. Casas-Sainz, and J. J. Villala!ın (2012), Switch of Mesozoic extensional tectonic style in the Lusitanian basin (Portugal): Insights from magnetic fabrics, Tectonophysics, 536-537, 122–135, doi:10.1016/j.tecto.2012.03.010.

Soto, R., E. Beamud, B. Oliva-Urcia, and E. Roca (2014), Applicability of magnetic fabrics in rocks associated with the emplacement of salt structures (the Bicorb–Quesa and Navarr!es salt walls, Prebetics, SE Spain), Tectonophysics, 629, 319–334.

Visiting Fellow Reports

Evaluating paramagnetic anisotropy through low temperature susceptibility measurements.

Ran Issachar
Tel Aviv University, Israel
ranissachar@gmail.com

We studied the magnetic fabrics (i.e. AMS) of carbonate samples from the deformation zone of the Dead Sea Fault plate boundary, Israel. These samples display the competing effect of paramagnetic and diamagnetic minerals, so that the mean susceptibility (km) is close to zero (1 to 25 .10-6SI). In order to enhance the paramagnetic anisotropy we took advantage of the susceptibility increase at low temperatures (Curie-Weiss law). We examined two approaches: (1) measuring the full susceptibility tensor at a constant temperature of ~77K (LT-AMS) and (2) measuring susceptibility versus temperature curves, between 20K to room temperature, for two orthogonal sample orientations.

In the first approach, we measured the LT-AMS using the MFK Kappabridge, after the samples were cooled in a liquid nitrogen bath. We followed the protocol of Lüneburg et al. (1999) that was further developed by Oliva-Urcia et al. (2010) and Issachar et al. (2016). We compared the manual and spinning holder methods and found that the spinning holder method is more precise. We formulated a technical protocol for the low temperature measurements (see companion article in this Quarterly issue). The results reveal that the LT-AMS differs from the room temperature AMS (RT-AMS) (Figure 1). Mean susceptibility values increased dramatically, by factor of 4.5 to 20. The minimum susceptibility axes (k3) are more clustered and vertically oriented. The maximum (k1) and intermediate (k2) axes are more horizontally foliated. Moreover, the shape of the anisotropy at LT-AMS is constantly oblate (T≈1) and the anisotropy degree (P) is lower than RT-AMS and relatively constant between samples of same site. The LT-AMS fabrics are comparable to fabrics resulting from depositional and compaction processes (Parés et al., 1999; Aubourg et al., 2004).

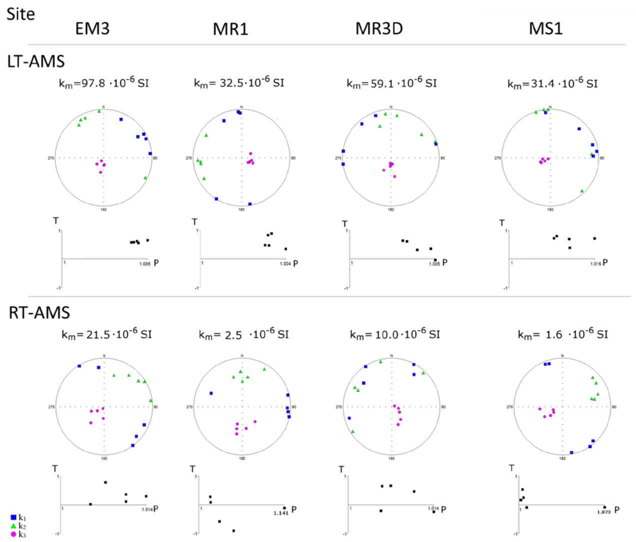

Figure 1. LT-AMS and RT-AMS results of four sampling sites within the DSF plate boundary. km is average mean susceptibility. Stereograms are lower-hemisphere, equal-area projection of principal susceptibilities axes maximum (blue), intermediate (green) and minimum (pink). The graphs shows shape of anisotropy (T) versus anisotropy degree (P).

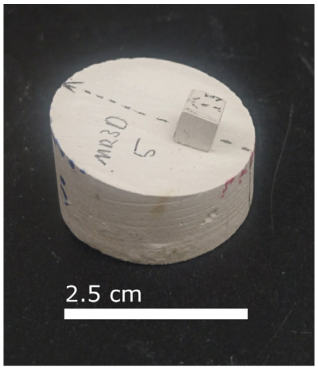

Figure 2. 4mm cube specimen cut along the principal susceptibility axes.

In the second approach, orientation dependent k(T) curves (susceptibility versus temperature) were measured, from 20K to room temperature. Small cubes (~4mm) were cut from the cylindrical samples in such a way that the faces of the cubes are perpendicular to the RT-AMS principal susceptibilities (Figure 2).

Using the MPMS instrument, *k*(T) curves were measured along the k1 and along k3 directions separately. The hypothesis was that if paramagnetic minerals are the source of anisotropy in the sample, then the anisotropy degree (P = k1/k3) will inversely increase with temperature. This approach was also performed by Biedermann et al. (2014 a,b). The advantages are the ability to perform measurements at very low temperatures (close to

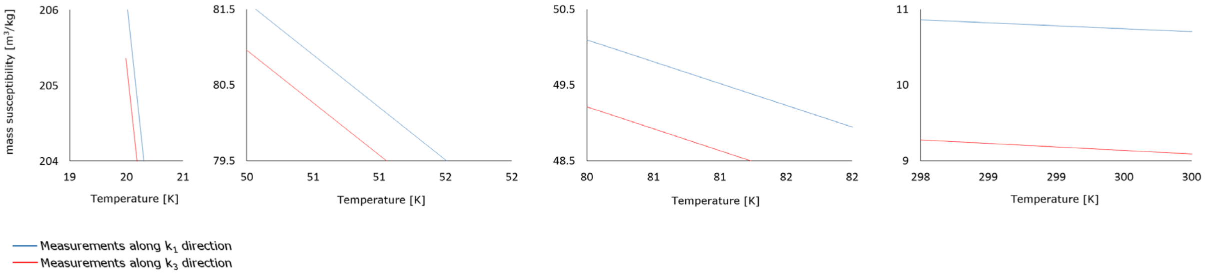

Figure 3. *k*(T) curves of a sample from EP site.

absolute zero), high accuracy, and high certainty regarding measurement temperature. The disadvantages are reduced sample volume and difficulties in precisely orienting the samples. Figure 3 shows the results for one specimen. Unfortunately the results are unreliable. The P values obtained at room temperature did not match the values obtained by RT-AMS. Furthermore, for some specimens the susceptibility along the k1 direction was lower than along the k3 direction, indicating a fundamental problem in the experiment design. We suggest that tiny differences in sample positioning within the coil between the two curves (namely differences in centering) would lead to differences in the measured susceptibility, which are greater than the expected anisotropy degree. Therefore, although the greater measurement precision, a direct comparison between the two curves is unreliable.

References

Aubourg, C., Smith, B., Bakhtari, H., Guya, N., Eshragi, A., Lallemant, S., ... & Delaunay, S. (2004). Post-Miocene shortening pictured by magnetic fabric across the Zagros-Makran syntaxis (Iran). Geological Society of America Special Papers, 383, 17-40.

Biedermann, A. R., Koch, C. B., Lorenz, W. E., & Hirt, A. M. (2014a). Low-temperature magnetic anisotropy in micas and chlorite. Tectonophysics, 629, 63-74.

Biedermann, A. R., Pettke, T., Reusser, E., & Hirt, A. M. (2014b). Anisotropy of magnetic susceptibility in natural olivine single crystals. Geochemistry, geophysics, geosystems, 15(7), 3051-3065.

Issachar, R., T. Levi, V. Lyakhovsky, S. Marco, and R. Weinberger (2016), Improving the method of low temperature anisotropy of magnetic susceptibility (LT-AMS) measurements in air, Geochem. Geophys. Geosyst., 17, 2940–2950, doi:10.1002/2016GC006339.

Lüneburg, C. M., Lampert, S. A., Lebit, H. D., Hirt, A. M., Casey, M., & Lowrie, W. (1999). Magnetic anisotropy, rock fabrics and finite strain in deformed sediments of SW Sardinia (Italy). Tectonophysics, 307(1-2), 51-74.

Oliva-Urcia, B., Rahl, J. M., Schleicher, A. M., & Parés, J. M. (2010). Correlation between the anisotropy of the magnetic susceptibility, strain and X-ray Texture Goniometry in phyllites from Crete, Greece. Tectonophysics, 486(1), 120-131.

Parés, J. M., van der Pluijm, B. A., & Dinarès-Turell, J. (1999). Evolution of magnetic fabrics during incipient deformation of mudrocks (Pyrenees, northern Spain). Tectonophysics, 307(1), 1-14.

Rock Magnetic Analysis of the early Paleocene Upper Nacimiento Formation, San Juan Basin, New Mexico

Caitlin Leslie
Baylor University, Waco, TX
Caitlin_Leslie@baylor.edu

The San Juan Basin in New Mexico contains extensive outcrops of alluvial foreland basin deposits with a robust record of early Paleocene mammalian evolution within the Nacimiento Formation. Work is ongoing to reconstruct the depositional environments and climate through time to understand the potential extrinsic controls on mammalian turnover between the Torrejonian 2 (To2) and Torrejonian 3 (To3) North American Land Mammal Ages (NALMA). An essential part of this research is creating a precise chronostratigraphic framework for

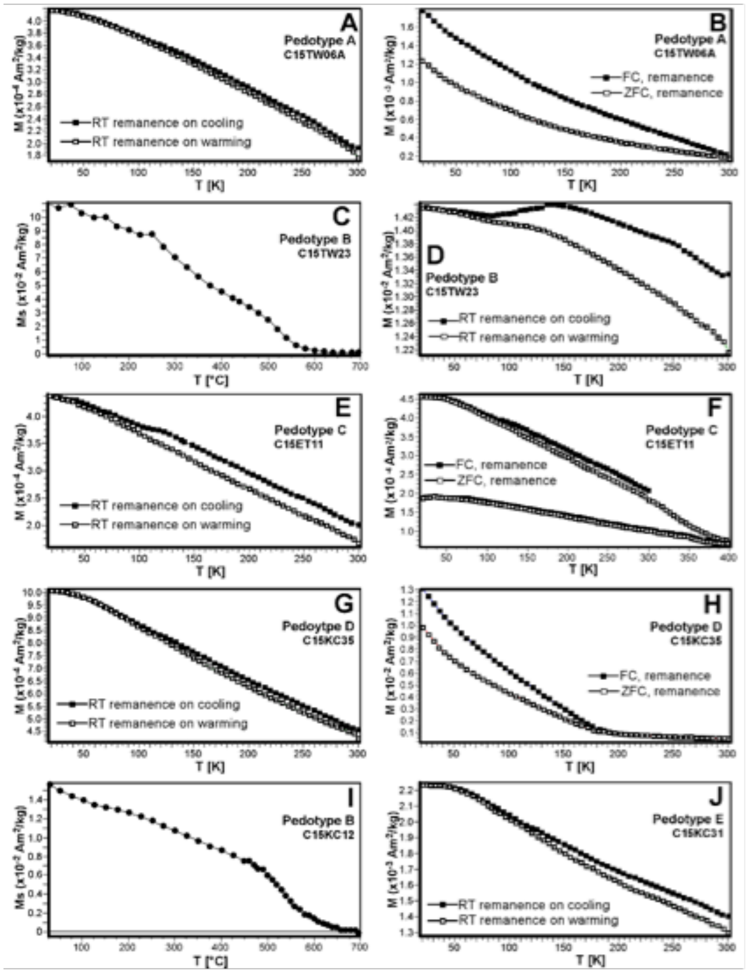

Figure 1. Rock magnetic analyses for representative lithologies of the Upper Nacimiento Formation.

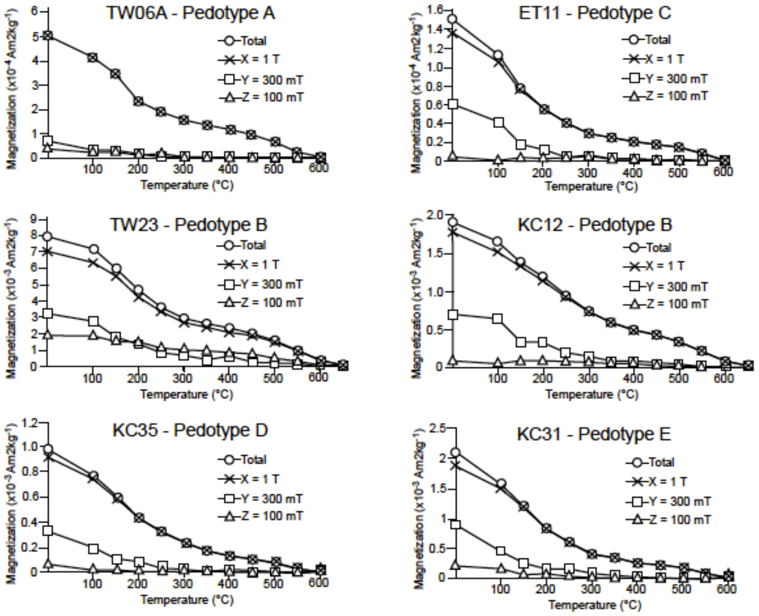

Figure 2. Thermal demagnetization of orthogonal isothermal remanent magnetizations for six specimens.

these deposits using magnetostratigraphy to calculate sedimentation rates, constrain mammal locality ages, and document the timing of climate changes.

Understanding the dominant magnetic carriers is important to accurately interpret the paleomagnetic data and fully characterize the deposits. Rock magnetic analyses by Butler and Lindsay (1985) documented intermediate composition titanohematite as the dominant ferrimagnetic mineral from nine stratigraphic levels throughout the Late Cretaceous to middle Paleocene deposits in the San Juan Basin. Given the broad spacing of their sampling, it is unclear if any samples overlap with the study interval presented here and fully characterize the deposits.

To characterize the magnetic mineralogies and assess whether titanohematite was the primary magnetic carrier, I visited the IRM to use the Kappabridge, high temperature VSM, and MPMS. Representative samples were run for each analyses which involved lumping the various paleosols throughout the formation into representative pedotypes.

Rock magnetic analyses show that the Upper Nacimiento has a mixed magnetic mineralogy. Low temperature magnetometry for a representative sample of Pedotype A (black, slickensided paleosol) shows a two-fold increase on warming, the Verwey transition, and possibly the Morin transition (when evaluating the derivatives of the RTSIRM and FC-ZFC curves) indicating goethite, magnetite, and hematite are present (Fig. 1A and 1B). Pedotype B samples (red, calcareous paleosol) suggest goethite, titanomagnetite, maghemite, and hematite from high temperature susceptibility and low temperature magnetometry measurements (Fig. 1C, 1D, and 1I). Low temperature magnetrometry measurements from a Pedotype C sample (brown, weakly-developed paleosol) show a Verwey transition indicating magnetite (Fig. 1E). A goethite test performed using low temperature magnetrometry indicates the presence of goethite along with another high-coercivity carrier after the goethite is demagnetized at 400 K, likely titanohematite (Fig 1F). RTSIRM curves for a representative sample from Pedotype D (tan, weakly-developed paleosol) suggest magnetite, supported by the presence of the Verwey transition (Fig. 1G). FC-ZFC-LTSIRM curves converge at 190 K which indicates Al-substituted goethite is present (Fig 1H). RTSIRM curves for a Pedotype G sample (tan, silty paleosol) have a separation at 90 K indicating titanomagnetite and a slight Morin transition indicating hematite (Fig. 1J).

Triaxial-IRM Lowrie tests were necessary to determine the primary magnetic carrier in each sample, given the evidence for multiple mineralogies outlined above. For all samples analyzed the majority of the IRM is held by grains whose coercivities are greater than 1 T (Fig. 2). The largest remanence drop occurs between 100-150°C suggesting goethite is the primary carrier. Some samples also show a decrease in remanence between 150-200°C suggesting titanohematite may also be present. Remanence remaining after 200°C is likely held by pigmentary hematite for samples TW23 and KC12, supported by the loss of remanence between 600-650°C, red coloring, and the low temperature rock magnetrometry experiments. In all other samples, the remaining remanence is likely maghemite that converted to hematite with heating. All samples except TW06A also show remanence held by the 300 mT curve up to ~300°C, supporting the presence of magnetite/maghemite.

Rock magnetic experiments performed while visiting the IRM helped determined that the Upper Nacimiento Formation has a mixed magnetic mineralogy with goethite as the dominant carrier. Although titanohematite is likely present in most samples, and together with magnetite constitutes the primary mineralogy, it does not appear to be the dominant remanence carrier. These results helped with interpretation of the paleomagnetic data which is a critical part of the broader research goals of understanding environmental, climatic, and biotic changes over this time interval.

Acknowledgements:

I would like to thank Dario Bilardello, Mike Jackson, and Peat Solheid for assistance and guidance at the IRM. This study was funded by an IRM Visiting Student Fellowship, NSF EAR-132552, ACS-PRF #52822-DN18, SEPM, Colorado Scientific Society, Fort Worth Geological Society, and Baylor University.

References:

Butler, R.F. and E.H. Lindsay. 1985. Mineralogy of magnetic minerals and revised magnetic polarity stratigraphy of continental sediments, San Juan Basin, New Mexico. Journal of Geology 93: 535-554.

Current Articles

A list of current research articles dealing with various topics in the physics and chemistry of magnetism is a regular feature of the IRM Quarterly. Articles published in familiar geology and geophysics journals are included; special emphasis is given to current articles from physics, chemistry, and materials-science journals. Most are taken from ISI Web of Knowledge, after which they are subjected to Procrustean culling for this newsletter. An extensive reference list of articles (primarily about rock magnetism, the physics and chemistry of magnetism, and some paleomagnetism) is continually updated at the IRM. This list, with more than 10,000 references, is available free of charge. Your contributions both to the list and to the Current Articles section of the IRM Quarterly are always welcome.

Aeromagnetism, Magnetic Anomalies, and Surveying

Afshar, A., G. H. Norouzi, A. Moradzadeh, M. A. Riahi, and S. Porkhial (2017), Curie Point Depth, Geothermal Gradient and Heat-Flow Estimation and Geothermal Anomaly Exploration from Integrated Analysis of Aeromagnetic and Gravity Data on the Sabalan Area, NW Iran, Pure and Applied Geophysics, 174(3), 1133-1152.

Austin, J. R., S. Schmid, and C. A. Foss (2017), Using stratiform magnetic anomalies to map near-surface architecture: insights from the Amadeus Basin, Australian Journal of Earth Sciences, 64(3), 353-383.

Azeez, K. K. A., P. K. Patro, T. Harinarayana, and S. V. S. Sarma (2017), Magnetotelluric imaging across the tectonic structures in the eastern segment of the Central Indian Tectonic Zone: Preserved imprints of polyphase tectonics and evidence for suture status of the Tan Shear, Precambrian Research, 298, 325-340.

Balkaya, C., Y. L. Ekinci, G. Gokturkler, and S. Turan (2017), 3D non-linear inversion of magnetic anomalies caused by prismatic bodies using differential evolution algorithm, Journal of Applied Geophysics, 136, 372-386.

Beka, T. I., K. Senger, U. A. Autio, M. Smirnov, and Y. Birkelund (2017), Integrated electromagnetic data investigation of a Mesozoic CO2 storage target reservoir-cap-rock succession, Svalbard, Journal of Applied Geophysics, 136, 417-430.

Blanchard, J. A., R. E. Ernst, and C. Samson (2017), Gravity and magnetic modelling of layered mafic-ultramafic intrusions in large igneous province plume centre regions: case studies from the 1.27 Ga Mackenzie, 1.38 Ga Kunene-Kibaran, 0.06 Ga Deccan, and 0.13-0.08 Ga High Arctic events, Canadian Journal of Earth Sciences, 54(3), 290-310.

Corseri, R., K. Senger, K. Selway, M. M. Abdelmalak, S. Planke, and D. A. Jerram (2017), Magnetotelluric evidence for massive sulphide mineralization in intruded sediments of the outer Voring Basin, mid-Norway, Tectonophysics, 706, 196-205.

Damaceno, J. G., D. L. de Castro, S. N. Valcacio, and Z. S. Souza (2017), Magnetic and gravity modeling of a Paleogene diabase plug in Northeast Brazil, Journal of Applied Geophysics, 136, 219-230.

Gailler, L., and J. Kauahikaua (2017), Monitoring the cooling of the 1959 Kilauea Iki lava lake using surface magnetic measurements, Bulletin of Volcanology, 79(6).

Gailler, L., D. Arcay, P. Munch, G. Martelet, I. Thinon, and J. F. Lebrun (2017), Forearc structure in the Lesser Antilles inferred from depth to the Curie temperature and thermo-mechanical simulations, Tectonophysics, 706, 71-90.

Knicely, J., M. E. Everett, and D. W. Sparks (2017), Magnetic anomalies on Io and their relationship to the spatial distribution of volcanic centers, Physics of the Earth and Planetary Interiors, 269, 133-147.

Liu, S., X. Y. Hu, J. C. Cai, J. H. Li, C. L. Shan, W. Wei, Q. Han, and Y. J. Liu (2017), Inversion of borehole magnetic data for prospecting deep-buried minerals in areas with near-surface magnetic distortions: a case study from the Daye iron-ore deposit in Hubei, central China, Near Surface Geophysics, 15(3), 298-310.

Mansi, A. H., S. Marzi, E. Farshchiansadegh, and G. Bernasconi (2017), Sensitivity analysis of marine Controlled-Source Electromagnetic data, Bollettino Di Geofisica Teorica Ed Applicata, 58(1), 43-54.

Menezes, P. T. L., J. M. Travassos, A. J. A. Marcal, and F. A. M. Santos (2017), 3D magnetotelluric exploration of Sete Cidades Volcano, Sao Miguel Island, Azores, Interpretation-a Journal of Subsurface Characterization, 5(2), T219-T230.

Mousa, A., K. Mickus, and A. Al-Rahim (2017), The thickness of cover sequences in the Western Desert of Iraq from a power spectrum analysis of gravity and magnetic data, Journal of Asian Earth Sciences, 138, 230-245.

Nam, M. J., Y. Song, H. Jang, and B. Kim (2017), 4D inversion of time-lapse magnetotelluric data sets for monitoring geothermal reservoir, Journal of Applied Geophysics, 141, 88-97.

Pathak, A. K., M. Sridhar, Y. Harsha, A. Markandeyulu, B. Raju, and A. K. Chaturvedi (2017), East-West Mafic Dyke in Aravallis - A Post-depositional Event Deciphered by Aeromagnetic Studies, Journal of the Geological Society of India, 89(6), 675-678.

Pedrosa, N. C., R. M. Vidotti, R. A. Fuck, R. Branco, A. R. de Almeida, N. C. V. Silva, and L. R. C. Braga (2017), Architecture of the intracontinental Jaibaras Rift, Brazil, based on geophysical data, Journal of South American Earth Sciences, 74, 27-40.

Percival, J. A., and V. Tschirhart (2017), Trans-Hudsonian far-field deformation effects in the Rae foreland: An integrated geological-3D magnetic model, Tectonophysics, 699, 82-92.

Suzuki, K., Y. Kusano, R. Ochi, N. Nishiyama, T. Tokunaga, and K. Tanaka (2017), Electromagnetic exploration in high-salinity groundwater zones: case studies from volcanic and soft sedimentary sites in coastal Japan, Exploration Geophysics, 48(2), 95-109.

Szitkar, F., M. A. Tivey, D. S. Kelley, J. A. Karson, G. L. Fruh-Green, and A. R. Denny (2017), Magnetic exploration of a low-temperature ultramafic-hosted hydrothermal site (Lost City, 30 degrees N, MAR), Earth and Planetary Science Letters, 461, 40-45.

Teknik, V., and A. Ghods (2017), Depth of magnetic basement in Iran based on fractal spectral analysis of aeromagnetic data, Geophysical Journal International, 209(3), 1878-1891.

Tschirhart, V., C. W. Jefferson, and W. A. Morris (2017), Basement geology beneath the northeast Thelon Basin, Nunavut: insights from integrating new gravity, magnetic and geological data, Geophysical Prospecting, 65(2), 617-636.

Usui, Y., Y. Ogawa, K. Aizawa, W. Kanda, T. Hashimoto, T. Koyama, Y. Yamaya, and T. Kagiyama (2017), Three-dimensional resistivity structure of Asama Volcano revealed by data-space magnetotelluric inversion using unstructured tetrahedral elements, Geophysical Journal International, 208(3), 1359-1372.

Wang, X. J., L. F. He, L. Chen, L. G. Xu, J. Li, X. Y. Lei, and D. H. Wei (2017), Mapping deeply buried karst cavities using controlled-source audio magnetotellurics: A case history of a tunnel investigation in southwest China, Geophysics,

82(1), EN1-EN11.

Xu, Y., T. Y. Hao, H. Zeyen, and F. Z. Nan (2017), Curie Point Depths in North China Craton Based on Spectral Analysis of Magnetic Anomalies, Pure and Applied Geophysics, 174(1), 339-347.

Archeomagnetism

Carrancho, A., A. Goguitchaichvili, J. Morales, J. A. Espinosa-Soto, J. J. Villalain, J. L. Arsuaga, E. Baquedano, and A. Perez-Gonzalez (2017), Full-vector archaeomagnetic dating of a medieval limekiln at Pinilla del Valle site (Magrid, Spain), Archaeometry, 59(2), 373-394.

Costanzo-Alvarez, V., R. Devesa-Rey, M. Aldana, M. T. Barral, D. Lopez-Rodriguez, and B. Andrade (2017), Magnetic properties of surface sediments as proxies of recent anthropogenic pollution in the Anllons riverbed (NW Spain), Environmental Earth Sciences, 76(13).

Li, X. W., H. Ao, M. J. Dekkers, A. P. Roberts, P. Zhang, S. Lin, W. W. Huang, Y. M. Hou, W. H. Zhang, and Z. S. An (2017), Early Pleistocene occurrence of Acheulian technology in North China, Quaternary Science Reviews, 156, 12-22.

Lopez-Sanchez, J., G. McIntosh, M. L. Osete, A. del Campo, J. J. Villalain, L. Perez, M. Kovacheva, and O. R. de la Fuente (2017), Epsilon iron oxide: Origin of the high coercivity stable low Curie temperature magnetic phase found in heated archeological materials, Geochemistry Geophysics Geosystems, 18(7), 2646-2656.

Martin, F. F., A. Di Piazza, C. D'Oriano, M. L. Carapezza, A. Paonita, S. G. Rotolo, and L. Sagnotti (2017), New insights into the provenance of the obsidian fragments of the island of Ustica (Palermo, Sicily), Archaeometry, 59(3), 435-454.

Matasova, G. G., A. Y. Kazansky, N. O. Kozhevnikov, S. V. Snpokov, and A. V. Kharinsky (2017), A rock-magnetic quest for possible ore sources for the ancient iron-smelting industry in the Olkhon region (Lake Baikal, Siberia), Archaeometry, 59(3), 511-527.

Morales, J., M. D. Hernandez-Bernal, A. Goguitchaichvili, and J. L. Punzo-Diaz (2017), An integrated magnetic, geochemical and archeointensity investigation of casting debris from ancient metallurgical sites of Michoacan, Western Mesoamerica, Studia Geophysica Et Geodaetica, 61(2), 290-309.

Biomagnetism

Blinova, I., L. Kanarbik, N. Irha, and A. Kahru (2017), Ecotoxicity of nanosized magnetite to crustacean Daphnia magna and duckweed Lemna minor, Hydrobiologia, 798(1), 141-149.

Till, J. L., Y. Guyodo, F. Lagroix, G. Morin, N. Menguy, and G. Ona-Nguema (2017), Presumed magnetic biosignatures observed in magnetite derived from abiotic reductive alteration of nanogoethite, Comptes Rendus Geoscience, 349(2), 63-70.

Computing and Techniques

Davis, J. R., and S. J. Titus (2017), Modern methods of analysis for three-dimensional orientational data, Journal of Structural Geology, 96, 65-89.

Iaffaldano, G., and S. Stein (2017), Impact of uncertain reference-frame motions in plate kinematic reconstructions: A theoretical appraisal, Earth and Planetary Science Letters, 458, 349-356.

Lerner, G. A., A. V. Smirnov, L. V. Surovitckii, and E. J. Piispa (2017), Nonheating methods for absolute paleointensity determination: Comparison and calibration using synthetic and natural magnetite-bearing samples, Journal of Geophysical Research-Solid Earth, 122(3), 1614-1633.

Morzfeld, M., A. Fournier, and G. Hulot (2017), Coarse predictions of dipole reversals by low-dimensional modeling and data assimilation, Physics of the Earth and Planetary Interiors, 262, 8-27.

Nabert, C., D. Heyner, and K. H. Glassmeier (2017), Estimation of a planetary magnetic field using a reduced magnetohydrodynamic model, Annales Geophysicae, 35(3), 465-474.

Panovska, S., and C. G. Constable (2017), An activity index for geomagnetic paleosecular variation, excursions, and reversals, Geochemistry Geophysics Geosystems, 18(4), 1366-1375.

Environmental magnetism and Climate

Anchuela, O. P., P. Frongia, F. Di Gregorio, A. M. C. Sainz, and A. P. Juan (2017), Magnetometry and ground-penetrating radar surveys applied to tracing potential collectors of mining-derived pollutants in coastal sediments (Piscinas Bay, Montevecchio mining area, SW Sardinia), Environmental Earth Sciences, 76(5).

Attoucheik, L., N. Jordanova, B. Bayou, F. Lagroix, D. Jordanova, S. Maouche, B. Henry, and A. Boutaleb (2017), Soil metal pollution from former Zn-Pb mining assessed by geochemical and magnetic investigations: case study of the Bou Caid area (Tissemsilt, Algeria), Environmental Earth Sciences, 76(7).

Badesab, F., T. von Dobeneck, R. M. Briggs, K. R. Bryan, J. Just, and H. Muller (2017), Sediment dynamics of an artificially deepened mesotidal coastal lagoon: An environmental magnetic investigation of Tauranga Harbour, New Zealand, Estuarine Coastal and Shelf Science, 194, 240-251.

Badesab, F., S. D. Iyer, A. R. Gujar, D. K. Naik, S. S. Gaonkar, R. A. A. Luis, P. Shirodkar, and S. Naik (2017), Understanding heavy mineral dynamics using magnetic fingerprinting technique: a case study of North Maharashtra Coast, India, Environmental Earth Sciences, 76(6).

Badesab, F., P. Dewangan, A. Usapkar, M. Kocherla, A. Peketi, K. Mohite, S. J. Sangode, and K. Deenadayalan (2017), Controls on evolution of gas-hydrate system in the Krishna-Godavari basin, offshore India, Geochemistry Geophysics Geosystems, 18(1), 52-74.

Bali, R., I. Khan, S. J. Sangode, A. K. Mishra, S. N. Ali, S. K. Singh, J. K. Tripathi, D. Sen Singh, and P. Srivastava (2017), Mid-to late Holocene climate response from the Triloknath palaeolake, Lahaul Himalaya based on multiproxy data, Geomorphology, 284, 206-219.

Bogalo, M. F., M. T. Ramirez-Herrera, A. Goguitchaichvili, D. Rey, K. J. Mohamed, M. Calvo-Rathert, and N. Corona (2017), Magnetic signature of the 22 June 1932 tsunami deposits (Jalisco, Mexican Pacific coast), Geochemistry Geophysics Geosystems, 18(6), 2370-2387.

Bohra, A., B. S. Kotlia, and N. Basavaiah (2017), Palaeoclimatic reconstruction by using the varvite sediments of Bharatpur, Upper Lahaul Valley, NW Himalaya, India, Quaternary International, 443, 39-48.

Bol'shakov, V. A. (2017), The Use of the Rock Magnetic and Paleomagnetic Data for the Loess Plateau Deposits in China for Their Climatologic and Chronologic Correlation to the Oxygen Isotopic Timescale, Izvestiya-Physics of the Solid Earth, 53(2), 293-310.

Chaparro, M. A. E., G. Suresh, V. Ramasamy, and M. Sundarrajan (2017), Magnetic assessment and pollution status of beach sediments from Kerala coast (southwestern India), Marine Pollution Bulletin, 117(1-2), 171-177.

Chen, Q. A., C. Kissel, and Z. F. Liu (2017), Late Quaternary climatic forcing on the terrigenous supply in the northern South China Sea: Input from magnetic studies, Earth and

Planetary Science Letters, 471, 160-171.

Chen, A. D., M. P. Zheng, L. F. Shi, H. L. Wang, and J. M. Xu (2017), Magnetostratigraphy of deep drilling core 15YZK01 in the northwestern Qaidam Basin (NE Tibetan Plateau): Tectonic movement, salt deposits and their link to Quaternary glaciation, Quaternary International, 436, 201-211.

Daradich, A., P. Huybers, J. X. Mitrovica, N. H. Chan, and J. Austermann (2017), The influence of true polar wander on glacial inception in North America, Earth and Planetary Science Letters, 461, 96-104.

Das, S. S., A. K. Singh, and N. Singh (2017), Provenance of bar-top Sediments at Tons River near Allahabad, Journal of the Geological Society of India, 89(5), 503-510.

Dutuc, D. C., G. Pe-Piper, and D. J. W. Piper (2017), The provenance of Jurassic and Lower Cretaceous clastic sediments offshore southwestern Nova Scotia, Canadian Journal of Earth Sciences, 54(1), 33-51.

Fang, Q., et al. (2017), Tectonic uplift-influenced monsoonal changes promoted hominin occupation of the Luonan Basin: Insights from a loess-paleosol sequence, eastern Qinling Mountains, central China, Quaternary Science Reviews, 169, 312-329.

Franciskovic-Bilinski, S., H. Bilinski, K. Maldini, S. Milovic, Q. Zhang, and E. Appel (2017), Chemical and magnetic tracing of coal slag pollutants in karstic river sediments, Environmental Earth Sciences, 76(14).

Gamboa, A., J. C. Montero-Serrano, G. St-Onge, A. Rochon, and P. A. Desiage (2017), Mineralogical, geochemical, and magnetic signatures of surface sediments from the Canadian Beaufort Shelf and Amundsen Gulf (Canadian Arctic), Geochemistry Geophysics Geosystems, 18(2), 488-512.

Grison, H., E. Petrovsky, A. Kapicka, and H. Hanzlikova (2017), Detection of the pedogenic magnetic fraction in volcanic soils developed on basalts using frequency-dependent magnetic susceptibility: comparison of two instruments, Geophysical Journal International, 209(2), 654-660.

Groening, J. A. A., V. Costanzo-Alvarez, M. Aldana, E. Carrillo, and F. Audemard (2017), Magnetic record of El Nino Southern Oscillation in Late Pleistocene sediments from Mucubaji lake (western Venezuela), Studia Geophysica Et Geodaetica, 61(2), 336-360.

Hirst, C., P. S. Andersson, S. Shaw, I. T. Burke, L. Kutscher, M. J. Murphy, T. Maximov, O. S. Pokrovsky, C. M. Morth, and D. Porcelli (2017), Characterisation of Fe-bearing particles and colloids in the Lena River basin, NE Russia, Geochimica Et Cosmochimica Acta, 213, 553-573.

Hofmann, F., B. Reichenbacher, and K. A. Farley (2017), Evidence for > 5 Ma paleo-exposure of an Eocene-Miocene paleosol of the Bohnerz Formation, Switzerland, Earth and Planetary Science Letters, 465, 168-175.

Hosek, J., P. Pokorny, J. Prach, L. Lisa, T. M. Grygar, I. Knesl, and J. Trubac (2017), Late Glacial erosion and pedogenesis dynamics: Evidence from high-resolution lacustrine archives and paleosols in south Bohemia (Czech Republic), Catena, 150, 261-278.

Hounslow, M., H. E. White, N. A. Drake, M. J. Salem, A. El-Hawat, S. J. McLaren, V. Karloukovski, S. R. Noble, and O. Hlal (2017), Miocene humid intervals and establishment of drainage networks by 23 Ma in the central Sahara, southern Libya, Gondwana Research, 45, 118-137.

Jouve, G., A. Lise-Pronovost, P. Francus, A. S. De Coninck, and P. S. Team (2017), Climatic influence of the latest Antarctic isotope maximum of the last glacial period (AIM4) on Southern Patagonia, Palaeogeography Palaeoclimatology Palaeoecology, 472, 33-50.

Karimi, A., G. H. Haghnia, S. Ayoubi, and T. Safari (2017), Impacts of geology and land use on magnetic susceptibility and selected heavy metals in surface soils of Mashhad plain, northeastern Iran, Journal of Applied Geophysics, 138, 127-134.

Kars, M., R. J. Musgrave, K. Kodama, A. S. Jonas, M. Bordiga, W. Ruebsam, M. J. Mleneck-Vautravers, and T. Bauersachs (2017), Impact of climate change on the magnetic mineral assemblage in marine sediments from Izu rear arc, NW Pacific Ocean, over the last 1 Myr, Palaeogeography Palaeoclimatology Palaeoecology, 480, 53-69.

Kayvantash, D., I. Cojan, C. Kissel, and C. Franke (2017), Magnetic fingerprint of the sediment load in a meander bend section of the Seine River (France), Geomorphology, 286, 14-26.

Kent, D. V., L. Lanci, H. P. Wang, and J. D. Wright (2017), Enhanced magnetization of the Marlboro Clay as a product of soil pyrogenesis at the Paleocene-Eocene boundary?, Earth and Planetary Science Letters, 473, 303-312.

Kissel, C., Z. F. Liu, J. H. Li, and C. Wandres (2017), Magnetic signature of river sediments drained into the southern and eastern part of the South China Sea (Malay Peninsula, Sumatra, Borneo, Luzon and Taiwan), Sedimentary Geology, 347, 10-20.

Kulgemeyer, T., H. Muller, T. von Dobeneck, K. R. Bryan, W. P. de Lange, and C. N. Battershill (2017), Magnetic mineral and sediment porosity distribution on a storm-dominated shelf investigated by benthic electromagnetic profiling (Bay of Plenty, New Zealand), Marine Geology, 383, 78-98.

Kumar, A., P. Srivastava, and N. K. Meena (2017), Late Pleistocene aeolian activity in the cold desert of Ladakh: A record from sand ramps, Quaternary International, 443, 13-28.

Laceby, J. P., O. Evrard, H. G. Smith, W. H. Blake, J. M. Olley, J. P. G. Minella, and P. N. Owens (2017), The challenges and opportunities of addressing particle size effects in sediment source fingerprinting: A review, Earth-Science Reviews, 169, 85-103.

Lahtinen, M., M. Oinonen, M. Tallavaara, J. W. P. Walker, and P. Rowley-Conwy (2017), The advance of cultivation at its northern European limit: Process or event?, Holocene, 27(3), 427-438.

Lecomte, K. L., A. M. Sarmiento, J. Borrego, and J. M. Nieto (2017), Rare earth elements mobility processes in an AMD-affected estuary: Huelva Estuary (SW Spain), Marine Pollution Bulletin, 121(1-2), 282-291.

Lewis, C. J., C. Sancho, E. V. McDonald, J. L. Pena-Monne, E. L. Pueyo, E. Rhodes, M. Calle, and R. Soto (2017), Post-tectonic landscape evolution in NE Iberia using staircase terraces: Combined effects of uplift and climate, Geomorphology, 292, 85-103.

Li, J. W., R. A. Gastaldo, J. Neveling, and J. W. Geissman (2017), Siltstones across the daptocephalus (dicynodon) and lystrosaurus assemblage zones, Karoo basin, South Africa, show no evidence for aridification, Journal of Sedimentary Research, 87(6), 653-671.

Li, W., Z. X. Hu, W. G. Zhang, R. Ji, and T. T. H. Nguyen (2017), Influence of provenance and hydrodynamic sorting on the magnetic properties and geochemistry of sediments of the Oujiang River, China, Marine Geology, 387, 1-11.

Liu, S. Z., W. Krijgsman, M. J. Dekkers, and D. Palcu (2017), Early diagenetic greigite as an indicator of paleosalinity changes in the middle Miocene Paratethys Sea of central Europe, Geochemistry Geophysics Geosystems, 18(7), 2634-2645.

Liu, Z. F., J. L. Ma, G. J. Wei, Q. S. Liu, Z. X. Jiang, X. Ding, S. S. Peng, T. Zeng, and T. P. Ouyang (2017), Magnetism of

a red soil core derived from basalt, northern Hainan Island, China: Volcanic ash versus pedogenesis, Journal of Geophysical Research-Solid Earth, 122(3), 1677-1696.

Lohr, S. C., D. T. Murphy, L. D. Nothdurft, R. Bolhar, S. Piazolo, and C. Siegel (2017), Maghemite soil nodules reveal the impact of fire on mineralogical and geochemical differentiation at the Earth's surface, Geochimica Et Cosmochimica Acta, 200, 25-41.

Madureira, P., et al. (2017), The 1998-2001 submarine lava balloon eruption at the Serreta ridge (Azores archipelago): Constraints from volcanic facies architecture, isotope geochemistry and magnetic data, Journal of Volcanology and Geothermal Research, 329, 13-29.

Maffini, M. N., D. F. Ducart, S. Radice, J. Coniglio, F. D'Eramo, M. Demartis, L. Pinotti, A. M. Silva, and C. L. B. Toledo (2017), Petrographic, spectral and magnetic susceptibility study of hydrothermal alteration associated with Pb-Zn-Cu-Ag-Au polymetallic deposits in the Sierra de Comechingones, Cordoba (Argentina), Estudios Geologicos-Madrid, 73(1).

Marynowski, L., A. Pisarzowska, A. Derkowski, M. Rakocinski, R. Szaniawski, J. Srodon, and A. S. Cohen (2017), Influence of palaeoweathering on trace metal concentrations and environmental proxies in black shales, Palaeogeography Palaeoclimatology Palaeoecology, 472, 177-191.

Matt, P., W. Powell, R. Volkert, M. Gorring, and A. Johnson (2017), Sedimentary exhalative origin for magnetite deposits of the New Jersey Highlands, Canadian Journal of Earth Sciences, 54(9), 1008-1023.

Mirzaee, E., S. Gitipour, M. Mousavi, and S. Amini (2017), Optimization of total petroleum hydrocarbons removal from Mahshahr contaminated soil using magnetite nanoparticle catalyzed Fenton-like oxidation, Environmental Earth Sciences, 76(4).

Mischel, S. A., D. Scholz, C. Spotl, K. P. Jochum, A. Schroder-Ritzrau, and S. Fiedler (2017), Holocene climate variability in Central Germany and a potential link to the polar North Atlantic: A replicated record from three coeval speleothems, Holocene, 27(4), 509-525.

Moulin, M., F. Fluteau, V. Courtillot, J. Marsh, G. Delpech, X. Quidelleur, and M. Gerard (2017), Eruptive history of the Karoo lava flows and their impact on early Jurassic environmental change, Journal of Geophysical Research-Solid Earth, 122(2), 738-772.

Mzuza, M. K., W. G. Zhang, F. Kapute, and J. R. Selemani (2017), Magnetic properties of sediments from the Pangani River Basin, Tanzania: Influence of lithology and particle size, Journal of Applied Geophysics, 143, 42-49.

Mzuza, M. K., Z. Weiguo, L. S. Chapola, M. Tembo, and F. Kapute (2017), Determining sources of sediments at Nkula Dam in the Middle Shire River, Malawi, using mineral magnetic approach, Journal of African Earth Sciences, 126, 23-32.

Pandey, S., and S. K. Parcha (2017), Provenance, tectonic setting and source-area weathering of the lower Cambrian sediments of the Parahio valley in the Spiti basin, India, Journal of Earth System Science, 126(2).

Rodriguez, J. A. B., J. A. P. Fernandez, A. R. Vega, F. D. L. Saucedo, and K. I. C. Carreon (2017), Magnetic susceptibility and natural gamma radioactivity as indirect proxies for characterization of sandstones and limestones of the Sabinas basin, Geofizika, 34(1), 19-43.

Roperch, P., J. Gattacceca, M. Valenzuela, B. Devouard, J. P. Lorand, C. Arriagada, P. Rochette, C. Latorre, and P. Beck (2017), Surface vitrification caused by natural fires in Late Pleistocene wetlands of the Atacama Desert, Earth and Planetary Science Letters, 469, 15-26.

Rouzaut, S., and M. J. Orgeira (2017), Influence of volcanic glass on the magnetic signal of different paleosols in Crdoba, Argentina, Studia Geophysica Et Geodaetica, 61(2), 361-384.

Sandeep, K., R. Shankar, A. K. Warrier, M. G. Yadava, R. Ramesh, R. A. Jani, Z. Weijian, and X. F. Lu (2017), A multi-proxy lake sediment record of Indian summer monsoon variability during the Holocene in southern India, Palaeogeography Palaeoclimatology Palaeoecology, 476, 1-14.

Sarmast, M., M. H. Farpoor, and I. E. Boroujeni (2017), Magnetic susceptibility of soils along a lithotoposequence in southeast Iran, Catena, 156, 252-262.

Swanson-Hysell, N. L., and F. A. Macdonald (2017), Tropical weathering of the Taconic orogeny as a driver for Ordovician cooling, Geology, 45(8), 719-722.

Wang, M. F., W. Wang, K. Liu, P. P. Michalak, K. T. Wei, and M. Y. Hue (2017), In-situ LA-ICP-MS trace elemental analyzes of magnetite: The Tieshan skarn Fe-Cu deposit, Eastern China, Chemie Der Erde-Geochemistry, 77(1), 169-181.

Zan, J. B., X. M. Fang, M. D. Yan, and B. S. Li (2017), New insights into the palaeoclimatic interpretation of the temperature dependence of the magnetic susceptibility and magnetization of Mid-Late Pleistocene loess/palaeosols in Central Asia and the Chinese Loess Plateau, Geophysical Journal International, 208(2), 663-673.

Zhao, H., Y. B. Sun, and X. K. Qiang (2017), Iron oxide characteristics of mid-Miocene Red Clay deposits on the western Chinese Loess Plateau and their paleoclimatic implications, Palaeogeography Palaeoclimatology Palaeoecology, 468, 162-172.

Zhao, L. L., H. L. Hong, Q. Fang, K. Yin, C. W. Wang, Z. H. Li, J. Torrent, F. Cheng, and T. J. Algeo (2017), Monsoonal climate evolution in southern China since 1.2 Ma: New constraints from Fe-oxide records in red earth sediments from the Shengli section, Chengdu Basin, Palaeogeography Palaeoclimatology Palaeoecology, 473, 1-15.

Extraterrestrial and Planetary Magnetism

Arkani-Hamed, J., and D. Boutin (2017), South Pole Aitken Basin magnetic anomalies: Evidence for the true polar wander of Moon and a lunar dynamo reversal, Journal of Geophysical Research-Planets, 122(6), 1195-1216.

Blukis, R., R. Ruffer, A. I. Chumakov, and R. J. Harrison (2017), A high spatial resolution synchrotron Mossbauer study of the Tazewell IIICD and Esquel pallasite meteorites, Meteoritics & Planetary Science, 52(5), 925-936.

Bryson, J. F. J., B. P. Weiss, R. J. Harrison, J. Herrero-Albillos, and F. Kronast (2017), Paleomagnetic evidence for dynamo activity driven by inward crystallisation of a metallic asteroid, Earth and Planetary Science Letters, 472, 152-163.

Garrick-Bethell, I., B. P. Weiss, D. L. Shuster, S. M. Tikoo, and M. M. Tremblay (2017), Further evidence for early lunar magnetism from troctolite 76535, Journal of Geophysical Research-Planets, 122(1), 76-93.

Girault, F., F. Perrier, M. Moreira, B. Zanda, P. Rochette, and Y. Teitler (2017), Effective radium-226 concentration in meteorites, Geochimica Et Cosmochimica Acta, 208, 198-219.

Hewins, R. H., et al. (2017), Regolith breccia Northwest Africa 7533: Mineralogy and petrology with implications for early Mars, Meteoritics & Planetary Science, 52(1), 89-124.

Kuchka, C. R., C. D. K. Herd, E. L. Walton, Y. Guan, and Y. Liu (2017), Martian low-temperature alteration materials in shock-melt pockets in Tissint: Constraints on their preservation in shergottite meteorites, Geochimica Et Cosmochimica Acta, 210, 228-246.

Marnocha, C. L. (2017), Rock Coatings and the Potential for

Life on Mars, Elements, 13(3), 187-191.

Matsumoto, M., K. Tomeoka, and Y. Seto (2017), Nepheline and sodalite in chondrules of the Ningqiang carbonaceous chondrite: Implications for a genetic relationship with those in the matrix, Geochimica Et Cosmochimica Acta, 208, 220-233.

Miller, K. E., D. S. Lauretta, H. C. Connolly, E. L. Berger, K. Nagashima, and K. Domanik (2017), Formation of unequilibrated R chondrite chondrules and opaque phases, Geochimica Et Cosmochimica Acta, 209, 24-50.

Nie, N. X., N. Dauphas, and R. C. Greenwood (2017), Iron and oxygen isotope fractionation during iron UV photo-oxidation: Implications for early Earth and Mars, Earth and Planetary Science Letters, 458, 179-191.

Oliveira, J. S., and M. A. Wieczorek (2017), Testing the axial dipole hypothesis for the Moon by modeling the direction of crustal magnetization, Journal of Geophysical Research-Planets, 122(2), 383-399.

Orgeira, M. J., et al. (2017), Extraterrestrial microspherules from Bajada del Diablo, Chubut, Argentina, Geoscience Frontiers, 8(1), 137-149.

Pignatelli, I., Y. Marrocchi, E. Mugnaioli, F. Bourdelle, and M. Gounelle (2017), Mineralogical, crystallographic and redox features of the earliest stages of fluid alteration in CM chondrites, Geochimica Et Cosmochimica Acta, 209, 106-122.

Reznik, B., A. Kontny, and J. Fritz (2017), Effect of moderate shock waves on magnetic susceptibility and microstructure of a magnetite-bearing ore, Meteoritics & Planetary Science, 52(7), 1495-1504.

Righter, K., B. M. Go, K. A. Pando, L. Danielson, D. K. Ross, Z. Rahman, and L. P. Keller (2017), Phase equilibria of a low S and C lunar core: Implications for an early lunar dynamo and physical state of the current core, Earth and Planetary Science Letters, 463, 323-332.

Sergienko, E. S., A. Kosterov, and P. V. Kharitonskii (2017), Two types of impact melts with contrasting magnetic mineralogy from Janisjarvi impact structure, Russian Karelia, Geophysical Journal International, 209(2), 1080-1094.

Szopa, K., T. Brachaniec, L. Karwowski, and T. Krzykawski (2017), Remnants of altered meteorite in the Cretaceous-Paleogene clay boundary in Poland, Meteoritics & Planetary Science, 52(4), 612-622.

Weiss, B. P., et al. (2017), A nonmagnetic differentiated early planetary body, Earth and Planetary Science Letters, 468, 119-132.

Fundamental Rock and Mineral Magnetism

Berndt, T., R. S. Ramalho, M. A. Valdez-Grijalva, and A. R. Muxworthy (2017), Paleomagnetic field reconstruction from mixtures of titanomagnetites, Earth and Planetary Science Letters, 465, 70-81.

Bompoti, N., M. Chrysochoou, and M. Machesky (2017), Surface structure of ferrihydrite: Insights from modeling surface charge, Chemical Geology, 464, 34-45.

Brok, E., C. Frandsen, K. Lefmann, S. McEnroe, P. Robinson, B. P. Burton, T. C. Hansen, and R. Harrison (2017), Spin orientation in solid solution hematite-ilmenite, American Mineralogist, 102(6), 1234-1243.

Ge, K. P., Q. S. Liu, J. Z. Deng, D. Nobes, Y. Wang, Y. G. Wang, and X. Chen (2017), Rock magnetic investigation and its geological significance for vein-type uranium deposits in southern China, Geochemistry Geophysics Geosystems, 18(4), 1333-1349.

Geuna, S., L. Escosteguy, B. D. Appella, F. D'Eramo, and L. Pinotti (2017), Magnetic susceptibility mapping of the Cambrian El Hongo pluton, Eastern Sierras Pampeanas, Argentina, Studia Geophysica Et Geodaetica, 61(2), 219-232.

Gomez Samus, M., Y. Rico, S. Ziccarelli, A. V. Parodi, and J. C. Bidegain (2017), Initial CaCO3 content effects in magnetic properties of calcined sediments. Preliminary results, Boletin De La Sociedad Geologica Mexicana, 69(1), 261-278.

Goncalves, E. C., P. N. da Silva, C. S. Silveira, G. Carneiro, A. B. Domingues, A. Moss, T. Pritchard, A. Plastino, and R. B. D. Azeredo (2017), Prediction of carbonate rock type from NMR responses using data mining techniques, Journal of Applied Geophysics, 140, 93-101.

Gribov, S. K., A. V. Dolotov, and V. P. Shcherbakov (2017), Experimental Modeling of the Chemical Remanent Magnetization and Thellier Procedure on Titanomagnetite-Bearing Basalts, Izvestiya-Physics of the Solid Earth, 53(2), 274-292.

Heinrich, F. C., V. Schmidt, M. Schramm, and M. Mertineit (2017), Magnetic and mineralogical properties of salt rocks from the Zechstein of the Northern German Basin, Geophysical Journal International, 208(3), 1811-1831.

Huang, W. T., P. C. Lippert, M. J. Jackson, M. J. Dekkers, Y. Zhang, J. Li, Z. J. Guo, P. Kapp, and D. J. J. van Hinsbergen (2017), Remagnetization of the Paleogene Tibetan Himalayan carbonate rocks in the Gamba area: Implications for reconstructing the lower plate in the India-Asia collision, Journal of Geophysical Research-Solid Earth, 122(2), 808-825.

Huang, W. T., P. C. Lippert, Y. Zhang, M. J. Jackson, M. J. Dekkers, J. Li, X. M. Hu, B. Zhang, Z. J. Guo, and D. J. J. van Hinsbergen (2017), Remagnetization of carbonate rocks in southern Tibet: Perspectives from rock magnetic and petrographic investigations, Journal of Geophysical Research-Solid Earth, 122(4), 2434-2456.

Kontny, A., and L. Grothaus (2017), Effects of shock pressure and temperature on titanomagnetite from ICDP cores and target rocks of the El'gygytgyn impact structure, Russia, Studia Geophysica Et Geodaetica, 61(1), 162-183.

Launay, N., P. Rochette, Y. Quesnel, F. Demory, N. S. Bezaeva, and D. Lattard (2017), Thermoremanence acquisition and demagnetization for titanomagnetite under lithospheric pressures, Geophysical Research Letters, 44(10), 4839-4845.

Li, Y. L., K. O. Konhauser, and M. G. Zhai (2017), The formation of magnetite in the early Archean oceans, Earth and Planetary Science Letters, 466, 103-114.

Morgan, S., R. Jones, J. Conner, J. Student, M. Schaner, E. Horsman, and M. de Saint Blanquat (2017), Magma sheets defined with magnetic susceptibility in the Maiden Creek sill, Henry Mountains, Utah, USA, Geology, 45(7), 599-602.

Phillips, S. C., J. E. Johnson, W. C. Clyde, J. B. Setera, D. P. Maxbauer, S. Severmann, and N. Riedinger (2017), Rock magnetic and geochemical evidence for authigenic magnetite formation via iron reduction in coal-bearing sediments offshore Shimokita Peninsula, Japan (IODP Site C0020), Geochemistry Geophysics Geosystems, 18(6), 2076-2098.

Robinson, P., S. A. McEnroe, and M. Jackson (2017), Lamellar magnetism and exchange bias in billion-year-old metamorphic titanohematite with nanoscale ilmenite exsolution lamellae - II: exchange-bias at 5 K after field-free cooling of NRM and after cooling in a+5 T field, Geophysical Journal International, 208(2), 895-917.

Sato, M., N. Mochizuki, M. Watanabe, and H. Tsunakawa (2017), Composition law of oblique anhysteretic remanent magnetization and its relation to the magnetostatic interaction, Geochemistry Geophysics Geosystems, 18(3), 1043-1052.

Soltis, J. A., A. M. Schwartzberg, P. Zarzycki, R. L. Penn, K.

M. Rosso, and B. Gilbert (2017), Electron Mobility and Trapping in Ferrihydrite Nanoparticles, Acs Earth and Space Chemistry, 1(4), 216-226.

Soumya, G. S., R. M. Asanulla, and T. Radhakrishna (2017), Rockmagnetism in relation to magnetic mineralogy of anorthosites in the southern granulite region of the Indian shield, Geophysical Journal International, 209(3), 1768-1778.

Spagnoli, G., A. Hordt, M. Jegen, C. Virgil, C. Rolf, and S. Petersen (2017), Magnetic susceptibility measurements of seafloor massive sulphide mini-core samples for deep-sea mining applications, Quarterly Journal of Engineering Geology and Hydrogeology, 50(1), 88-93.

Zhang, L., Z. M. Sun, H. B. Li, L. S. Zhao, S. R. Song, Y. M. Chou, Y. Cao, X. Z. Ye, H. Wang, and X. L. He (2017), Rock record and magnetic response to large earthquakes within Wenchuan Earthquake Fault Scientific Drilling cores, Geochemistry Geophysics Geosystems, 18(5), 1889-1906.

Geomagnetism

Arneitz, P., R. Egli, and R. Leonhardt (2017), Unbiased analysis of geomagnetic data sets and comparison of historical data with paleomagnetic and archeomagnetic records, Reviews of Geophysics, 55(1), 5-39.

Avery, M. S., J. S. Gee, and C. G. Constable (2017), Asymmetry in growth and decay of the geomagnetic dipole revealed in seafloor magnetization, Earth and Planetary Science Letters, 467, 79-88.

Bailey, R. L., T. S. Halbedl, I. Schattauer, A. Romer, G. Achleitner, C. D. Beggan, V. Wesztergom, R. Egli, and R. Leonhardt (2017), Modelling geomagnetically induced currents in midlatitude Central Europe using a thin-sheet approach, Annales Geophysicae, 35(3), 751-761.

Doumbia, V., K. Boka, N. Kouassi, O. D. F. Grodji, C. Amory-Mazaudier, and M. Menvielle (2017), Induction effects of geomagnetic disturbances in the geo-electric field variations at low latitudes, Annales Geophysicae, 35(1), 39-51.

Khokhlov, A., and G. Hulot (2017), On the cause of the non-Gaussian distribution of residuals in geomagnetism, Geophysical Journal International, 209(2), 1036-1047.

Landeau, M., J. Aubert, and P. Olson (2017), The signature of inner-core nucleation on the geodynamo, Earth and Planetary Science Letters, 465, 193-204.

Salminen, J., R. Klein, T. Veikkolainen, S. Mertanen, and I. Manttari (2017), Mesoproterozoic geomagnetic reversal asymmetry in light of new paleomagnetic and geochronological data for the Hame dyke swarm, Finland: Implications for the Nuna supercontinent, Precambrian Research, 288, 1-22.

Magnetic Fabrics and Anisotropy

Bhatt, S., V. Rana, and M. A. Mamtani (2017), Deciphering relative timing of fabric development in granitoids with similar absolute ages based on AMS study (Dharwar Craton, South India), Journal of Structural Geology, 94, 32-46.

Biedermann, A. R., M. Jackson, D. Bilardello, and S. A. McEnroe (2017), Effect of magnetic anisotropy on the natural remanent magnetization in the MCU IVe' layer of the Bjerkreim Sokndal Layered Intrusion, Rogaland, Southern Norway, Journal of Geophysical Research-Solid Earth, 122(2), 790-807.

Bradak-Hayashi, B., K. Tanigawa, M. Hyodo, and Y. Seto (2017), Magnetic fabric evidence for rapid, characteristic changes in the dynamics of the 2011 Tohoku-oki tsunami, Marine Geology, 387, 85-96.

Byerly, A., B. Tikoff, M. Kahn, B. Jicha, R. Gaschnig, and A. K. Fayon (2017), Internal fabrics of the Idaho batholith, USA, Lithosphere, 9(2), 283-298.

Casas-Sainz, A. M., T. Roman-Berdiel, B. Oliva-Urcia, C. Garcia-Lasanta, J. J. Villalain, L. Aldega, S. Corrado, C. Caricchi, C. Invernizzi, and M. C. Osacar (2017), Multidisciplinary approach to constrain kinematics of fault zones at shallow depths: a case study from the Cameros-Demanda thrust (North Spain), International Journal of Earth Sciences, 106(3), 1023-1055.

Cho, H., M. Son, Y. K. Sohn, and M. E. Park (2017), Magnetic fabric (anisotropy of magnetic susceptibility) constraints on emplacement mechanism of clastic dikes, Journal of Geophysical Research-Solid Earth, 122(5), 3306-3333.

Dawai, D., R. Tchameni, J. Bascou, S. A. Wangmene, P. M. F. Tchunte, and J. L. Bouchez (2017), Microstructures and magnetic fabrics of the Ngaoundere granite pluton (Cameroon): Implications to the late-Pan-African evolution of Central Cameroon Shear Zone, Journal of African Earth Sciences, 129, 887-897.

Gaudreau, E., D. Schneider, F. Lagroix, E. Cossette, and B. Grasemann (2017), Controls and implications of anisotropy across a strain gradient within granodiorite, Serifos, Greece, Journal of Geodynamics, 105, 11-26.

Hoyer, L., and M. K. Watkeys (2017), Using magma flow indicators to infer flow dynamics in sills, Journal of Structural Geology, 96, 161-175.

Hrouda, F., and J. Jezek (2017), Role of single-domain magnetic particles in creation of inverse magnetic fabrics in volcanic rocks: A mathematical model study, Studia Geophysica Et Geodaetica, 61(1), 145-161.

Hrouda, F., M. Chadima, J. Jezek, and J. Pokorny (2017), Anisotropy of out-of-phase magnetic susceptibility of rocks as a tool for direct determination of magnetic subfabrics of some minerals: an introductory study, Geophysical Journal International, 208(1), 385-402.

Kon, S., N. Nakamura, Y. Nishimura, K. Goto, and D. Sugawara (2017), Inverse magnetic fabric in unconsolidated sandy event deposits in Kiritappu Marsh, Hokkaido, Japan, Sedimentary Geology, 349, 112-119.

Malone, D. H., J. P. Craddock, M. D. Schmitz, S. Kenderes, B. Kraushaar, C. J. Murphey, S. Nielsen, and T. M. Mitchell (2017), Volcanic Initiation of the Eocene Heart Mountain Slide, Wyoming, USA, Journal of Geology, 125(4), 439-457.

Mamtani, M. A., V. Abhijith, S. Lahiri, V. Rana, S. Bhatt, S. Goswami, and A. R. Renjith (2017), Determining the reference frame for kinematic analysis in S-tectonites using AMS, Journal of the Geological Society of India, 90(1), 5-8.

Sangode, S. J., R. Sharma, R. Mahajan, N. Basavaiah, P. Srivastava, S. S. Gudadhe, D. C. Meshram, and M. Venkateshwarulu (2017), Anisotropy of Magnetic Susceptibility and Rock Magnetic Applications in the Deccan Volcanic Province based on some Case Studies, Journal of the Geological Society of India, 89(6), 631-642.

Siachoque, A., C. A. Salazar, and R. Trindade (2017), Emplacement and deformation of the A-type Madeira granite (Amazonian Craton, Brazil), Lithos, 277, 284-301.

Singh, R. K. B., A. K. Singh, K. Sen, and S. J. Sangode (2017), Detection of a weak late-stage deformation event in granitic gneiss through anisotropy of magnetic susceptibility: implications for tectonic evolution of the Bomdila Gneiss in the Arunachal Lesser Himalaya, Northeast India, Geological Magazine, 154(3), 476-490.

Soto, R., E. Beamud, E. Roca, E. Carola, and Y. Almar (2017), Distinguishing the effect of diapir growth on magnetic fabrics of syn-diapiric overburden rocks: Basque-Cantabrian basin, Northern Spain, Terra Nova, 29(3), 191-201.

Weinberger, R., T. Levi, G. I. Alsop, and S. Marco (2017), Kinematics of Mass Transport Deposits revealed by magnetic fabrics, Geophysical Research Letters, 44(15), 7743-7749.

Zavada, P., T. Calassou, K. Schulmann, F. Hrouda, P. Stipska, P. Hasalova, J. Mikova, T. Magna, and P. Mixa (2017), Magnetic fabric transposition in folded granite sills in Variscan orogenic wedge, Journal of Structural Geology, 94, 166-183.

Zhu, K. Y., M. Y. Li, L. F. Shentu, Z. Y. Shen, and Y. H. Yu (2017), Evaluation of a small-diameter sampling method in magnetic susceptibility, AMS and X-ray CT studies and its applications to mafic microgranular enclaves (MMEs) in granite, Journal of Volcanology and Geothermal Research, 341, 208-227.

Mineralogy, Petrology, Mineral Physics and Chemistry

Beard, J. S., and B. R. Frost (2017), The stoichiometric effects of ferric iron substitutions in serpentine from microprobe data, International Geology Review, 59(5-6), 541-547.

Borisov, A., H. Behrens, and F. Holtz (2017), Effects of strong network modifiers on Fe3+/Fe2+ in silicate melts: an experimental study, Contributions to Mineralogy and Petrology, 172(5).

Borsig, N., A. C. Scheinost, S. Shaw, D. Schild, and T. Neumann (2017), Uptake mechanisms of selenium oxyanions during the ferrihydrite-hematite recrystallization, Geochimica Et Cosmochimica Acta, 206, 236-253.

Evans, B. W., S. M. Kuehner, D. J. Joswiak, and G. Cressey (2017), Serpentine, Iron-rich Phyllosilicates and Fayalite Produced by Hydration and Mg Depletion of Peridotite, Duluth Complex, Minnesota, USA, Journal of Petrology, 58(3), 495-512.

Kabengi, N. J., M. Chrysochoou, N. Bompoti, and J. Di Kubicki (2017), An integrated flow microcalorimetry, infrared spectroscopy and density functional theory approach to the study of chromate complexation on hematite and ferrihydrite, Chemical Geology, 464, 23-33.

Katika, K., M. Saidian, M. Prasad, and I. L. Fabricius (2017), Low-Field NMR Spectrometry of Chalk and Argillaceous Sandstones: Rock-Fluid Affinity Assessed from T-1/T-2 Ratio, Petrophysics, 58(2), 126-140.

Kausik, R., K. Fellah, L. Feng, and G. Simpson (2017), High- and Low-Field NMR Relaxometry and Diffusometry of the Bakken Petroleum System, Petrophysics, 58(4), 341-351.

Kawasumi, S., and H. Chiba (2017), Redox state of seafloor hydrothermal fluids and its effect on sulfide mineralization, Chemical Geology, 451, 25-37.

Kim, Y., K. Yuan, B. R. Ellis, and U. Becker (2017), Redox reactions of selenium as catalyzed by magnetite: Lessons learned from using electrochemistry and spectroscopic methods, Geochimica Et Cosmochimica Acta, 199, 304-323.

Kubicki, J. D., D. Tunega, and S. Kraemer (2017), A density functional theory investigation of oxalate and Fe(II) adsorption onto the (010) goethite surface with implications for ligand- and reduction-promoted dissolution, Chemical Geology, 464, 14-22.

Luhmann, A. J., B. M. Tutolo, C. Y. Tan, B. M. Moskowitz, M. O. Saar, and W. E. Seyfried (2017), Whole rock basalt alteration from CO2-rich brine during flow-through experiments at 150 degrees C and 150 bar, Chemical Geology, 453, 92-110.

Luhmann, A. J., B. M. Tutolo, B. C. Bagley, D. F. R. Mildner, P. P. Scheuermann, J. M. Feinberg, K. Ignatyev, and W. E. Seyfried (2017), Chemical and physical changes during seawater flow through intact dunite cores: An experimental study at 150-200 degrees C, Geochimica Et Cosmochimica Acta, 214, 86-114.

Sievwright, R. H., J. J. Wilkinson, H. S. O'Neill, and A. J. Berry (2017), Thermodynamic controls on element partitioning between titanomagnetite and andesitic-dacitic silicate melts, Contributions to Mineralogy and Petrology, 172(8).

Strehlau, J. H., B. M. Toner, W. A. Arnold, and R. L. Penn (2017), Accessible reactive surface area and abiotic redox reactivity of iron oxyhydroxides in acidic brines, Geochimica Et Cosmochimica Acta, 197, 345-355.

Sun, S., and Y. L. Li (2017), Microstructures, crystallography and geochemistry of magnetite in 2500 to 2200 million-year-old banded iron formations from South Africa, Western Australia and North China, Precambrian Research, 298, 292-305.

Sun, S., and Y. L. Li (2017), Geneses and evolutions of iron-bearing minerals in banded iron formations of >3760 to ca. 2200 million-year-old: Constraints from electron microscopic, X-ray diffraction and Mossbauer spectroscopic investigations, Precambrian Research, 289, 1-17.

Tang, Q. Y., C. S. Li, Y. Tao, E. M. Ripley, and F. Xiong (2017), Association of Mg-rich Olivine with Magnetite as a Result of Brucite Marble Assimilation by Basaltic Magma in the Emeishan Large Igneous Province, SW China, Journal of Petrology, 58(4), 699-714.

Taylor, S. D., M. C. Marcano, and U. Becker (2017), A first principles investigation of electron transfer between Fe(II) and U(VI) on insulating Al- vs. semiconducting Fe-oxide surfaces via the proximity effect, Geochimica Et Cosmochimica Acta, 197, 305-322.

Tomaszewski, E. J., S. Lee, J. Rudolph, H. F. Xu, and M. Ginder-Vogel (2017), The reactivity of Fe(II) associated with goethite formed during short redox cycles toward Cr(VI) reduction under oxic conditions, Chemical Geology, 464, 101-109.

Ugwu, I. M., and D. M. Sherman (2017), Irreversibility of sorption of cobalt to goethite (alpha-FeOOH) and disparities in dissolution of aged synthetic Co-goethite, Chemical Geology, 467, 168-176.

Wen, G., J. W. Li, A. H. Hofstra, A. E. Koenig, H. A. Lowers, and D. Adams (2017), Hydrothermal reequilibration of igneous magnetite in altered granitic plutons and its implications for magnetite classification schemes: Insights from the Handan-Xingtai iron district, North China Craton, Geochimica Et Cosmochimica Acta, 213, 255-270.

Xu, H. F., S. Lee, and H. W. Xu (2017), Luogufengite: A new nano-mineral of Fe2O3 polymorph with giant coercive field, American Mineralogist, 102(4), 711-719.

Yin, S., C. Q. Ma, and P. T. Robinson (2017), Textures and high field strength elements in hydrothermal magnetite from a skarn system: Implications for coupled dissolution-reprecipitation reactions, American Mineralogist, 102(5), 1045-1056.

Paleointensity and records of the geomagnetic field

Chen, L., D. Heslop, A. P. Roberts, L. Chang, X. Zhao, H. V. McGregor, G. Marino, L. Rodriguez-Sanz, E. J. Rohling, and H. Palike (2017), Remanence acquisition efficiency in biogenic and detrital magnetite and recording of geomagnetic paleointensity, Geochemistry Geophysics Geosystems, 18(4), 1435-1450.

Irurzun, M. A., M. A. E. Chaparro, A. M. Sinito, C. S. G. Gogorza, H. Nunez, N. R. Nowaczyk, and H. N. Bohnel (2017), Relative palaeointensity and reservoir effect on Lake Esmeralda, Antarctica, Antarctic Science, 29(4), 356-368.

Kapper, L., J. Morales, M. Calvo-Rathert, A. Goguitchaichvili, V. Mejia, A. Caccavari, A. N. Guevara, and R. C. Ruiz

(2017), A paleointensity study of Cretaceous volcanic rocks from the Western Cordillera, Colombia, Studia Geophysica Et Geodaetica, 61(2), 264-289.

Okada, M., Y. Suganuma, Y. Haneda, and O. Kazaoka (2017), Paleomagnetic direction and paleointensity variations during the Matuyama-Brunhes polarity transition from a marine succession in the Chiba composite section of the Boso Peninsula, central Japan, Earth Planets and Space, 69.

Shcherbakova, V. V., A. J. Biggin, R. V. Veselovskiy, A. V. Shatsillo, L. M. A. Hawkins, V. P. Shcherbakov, and G. V. Zhidkov (2017), Was the Devonian geomagnetic field dipolar or multipolar? Palaeointensity studies of Devonian igneous rocks from the Minusa Basin (Siberia) and the Kola Peninsula dykes, Russia, Geophysical Journal International, 209(2), 1265-1286.

Veikkolainen, T., M. Heimpel, M. E. Evans, L. J. Pesonen, and K. Korhonen (2017), A paleointensity test of the geocentric axial dipole (GAD) hypothesis, Physics of the Earth and Planetary Interiors, 265, 54-61.

Zhidkov, G. V., V. P. Shcherbakov, A. V. Dolotov, M. A. Smirnov, A. A. Ovsyannikov, and P. Y. Plechov (2017), Test determinations of paleointensity in historical lavas of Kamchatka, Izvestiya-Physics of the Solid Earth, 53(1), 162-172.

Paleomagnetism

Achaga, R. V., M. A. Irurzun, C. S. G. Gogorza, A. Goguitchaichvili, J. Morales, D. Loponte, and A. M. Sinito (2017), Paleomagnetic and paleoclimatic investigation at Laguna Melincue (Pampean Plains, Argentina): preliminary results, Studia Geophysica Et Geodaetica, 61(2), 318-335.

Agro, A., E. Zanella, J. L. Le Pennec, and A. Temel (2017), Complex remanent magnetization in the Kizilkaya ignimbrite (central Anatolia): Implication for paleomagnetic directions, Journal of Volcanology and Geothermal Research, 336, 68-80.

Alva-Valdivia, L. M., A. Agarwal, C. Caballero-Miranda, B. I. Garcia-Amador, W. Morales-Barrera, S. Rodriguez-Elizarraraz, and A. Rodriguez-Trejo (2017), Paleomagnetic and AMS studies of the El Castillo ignimbrite, central-east Mexico: Source and rock magnetic nature, Journal of Volcanology and Geothermal Research, 336, 140-154.

Berra, F., A. Zanchi, L. Angiolini, D. Vachard, G. Vezzoli, S. Zanchetta, M. Bergomi, H. R. Javadi, and M. Kouhpeyma (2017), The upper Palaeozoic Godar-e-Siah Complex of Jandaq: Evidence and significance of a North Palaeotethyan succession in Central Iran, Journal of Asian Earth Sciences, 138, 272-290.

Calvin, P., A. M. Casas-Sainz, J. J. Villalain, and B. Moussaid (2017), Diachronous folding and cleavage in an intraplate setting (Central High Atlas, Morocco) determined through the study of remagnetizations, Journal of Structural Geology, 97, 144-160.

Cao, Y., et al. (2017), New Late Cretaceous paleomagnetic data from volcanic rocks and red beds from the Lhasa terrane and its implications for the paleolatitude of the southern margin of Asia prior to the collision with India, Gondwana Research, 41, 337-351.

Cervantes-Solano, M., L. Kapper, A. Goguitchaichvili, V. C. Ruiz-Martinez, J. Rosas-Elguera, J. Morales, R. Maciel-Pena, and R. Cejudo-Ruiz (2017), A detailed paleomagnetic and rock-magnetic investigation around Cretaceous-Paleogene boundary: the Autlan (Western Mexico) volcanic sequence revisited, Studia Geophysica Et Geodaetica, 61(2), 233-248.

Di Chiara, A., T. Moncinhatto, C. H. Moreno, F. J. Pavon-Carrasco, and R. I. F. Trindade (2017), Paleomagnetic study of an historical lava flow from the Llaima volcano, Chile, Journal of South American Earth Sciences, 77, 141-149.

Evans, D. A. D., A. V. Smirnov, and A. P. Gumsley (2017), Paleomagnetism and U-Pb geochronology of the Black Range dykes, Pilbara Craton, Western Australia: a Neoarchean crossing of the polar circle, Australian Journal of Earth Sciences, 64(2), 225-237.

Eyster, A. E., R. R. Fu, J. V. Strauss, B. P. Weiss, C. F. Roots, G. P. Halverson, D. A. D. Evans, and F. A. Macdonald (2017), Paleomagnetic evidence for a large rotation of the Yukon block relative to Laurentia: Implications for a low-latitude Sturtian glaciation and the breakup of Rodinia, Geological Society of America Bulletin, 129(1-2), 38-58.

Fairchild, L. M., N. L. Swanson-Hysell, J. Ramezani, C. J. Sprain, and S. A. Bowring (2017), The end of Midcontinent Rift magmatism and the paleogeography of Laurentia, Lithosphere, 9(1), 117-133.

Fazzito, S. Y., A. E. Rapalini, J. M. Cortes, and C. M. Terrizzano (2017), Vertical-axis rotations and deformation along the active strike-slip El Tigre Fault (Precordillera of San Juan, Argentina) assessed through palaeomagnetism and anisotropy of magnetic susceptibility, International Journal of Earth Sciences, 106(2), 631-657.

Frank, U., N. R. Nowaczyk, T. Frederichs, and M. Korte (2017), Palaeo- and rock magnetic investigations on Late Quaternary sediments from low latitudes. I: geomagnetic palaeosecular variation and relative palaeointensity records from the Tobago Basin, Southeast Caribbean, Geophysical Journal International, 208(3), 1740-1755.

Franke, W., L. R. M. Cocks, and T. H. Torsvik (2017), The Palaeozoic Variscan oceans revisited, Gondwana Research, 48, 257-284.

Fu, R. R., et al. (2017), Evaluating the paleomagnetic potential of single zircon crystals using the Bishop Tuff, Earth and Planetary Science Letters, 458, 1-13.

Gallo, L. C., R. N. Tomezzoli, and E. O. Cristallini (2017), A pure dipole analysis of the Gondwana apparent polar wander path: Paleogeographic implications in the evolution of Pangea, Geochemistry Geophysics Geosystems, 18(4), 1499-1519.

Garcia-Lasanta, C., A. Casas-Sainz, J. J. Villalain, B. Oliva-Urcia, T. Mochales, and F. Speranza (2017), Remagnetizations used to unravel large-scale fold kinematics: A case study in the Cameros Basin (Northern Spain), Tectonics, 36(4), 714-729.

Garcia-Ruiz, R., A. Goguitchaichvili, H. L. Loera, M. Cervantes-Solano, J. Urrutia-Fucugauchi, J. Morales-Contreras, R. Maciel-Pena, and J. Rosas-Elguera (2017), Paleomagnetism and Aeromagnetic Survey From Tancitaro Volcano (Central Mexico) - Paleo-Secular Variation at Low Latitudes During the Past 1 Ma, Geofisica Internacional, 56(3), 287-304.

Garcia-Ruiz, R., A. Goguitchaichvili, M. Cervantes-Solano, J. Morales, R. Maciel-Pena, J. Rosas-Elguera, R. Cejudo-Ruiz, and J. Urrutia-Fucugauchi (2017), Rock-magnetic and paleomagnetic survey on dated lava flows erupted during the Bruhnes and Matuyama chrons: the Mascota Volcanic Field revisited (Western Mexico), Studia Geophysica Et Geodaetica, 61(2), 249-263.

Golovanova, I. V., K. N. Danukalov, A. F. Kadyrov, M. M. Khidiyatov, R. Y. Sal'manova, R. K. Shakurov, N. M. Levashova, and M. L. Bazhenov (2017), Paleomagnetism of Sedimentary Strata and the Origin of the Structures in the Western Slope of South Urals, Izvestiya-Physics of the Solid Earth, 53(2), 311-319.

Greve, A., and G. M. Turner (2017), New and revised palaeomagnetic secular variation records from post-glacial volcanic materials in New Zealand, Physics of the Earth and Planetary Interiors, 269, 1-17.

Henry, B., M. E. M. Derder, M. Amenna, S. Maouche, and B. Bayou (2017), Better constrained selection of the Paleozoic West Gondwana (South America) paleomagnetic poles for the APWP determination, Studia Geophysica Et Geodaetica, 61(2), 185-198.

Humbert, F., L. Sonnette, M. O. de Kock, P. Robion, C. S. Horng, A. Cousture, and H. Wabo (2017), Palaeomagnetism of the early Palaeoproterozoic, volcanic Hekpoort Formation (Transvaal Supergroup) of the Kaapvaal craton, South Africa, Geophysical Journal International, 209(2), 842-865.

Ingham, E., G. M. Turner, C. E. Conway, D. Heslop, A. P. Roberts, G. Leonard, D. Townsend, and A. Calvert (2017), Volcanic records of the Laschamp geomagnetic excursion from Mt Ruapehu, New Zealand, Earth and Planetary Science Letters, 472, 131-141.

Iosifidi, A. G., and V. A. Mikhailova (2017), Paleomagnetism of Carboniferous Formations of the Russian Platform: Reinvestigation of Old Collections, Izvestiya-Physics of the Solid Earth, 53(3), 461-476.

Kirscher, U., O. Oms, A. A. Bruch, I. Shatilova, G. Chochishvili, and V. Bachtadse (2017), The Calabrian in the Western Transcaucasian basin (Georgia): Paleomagnetic constraints from the Gurian regional stage, Quaternary Science Reviews, 160, 96-107.

Kovalenko, D. V. (2017), Paleomagnetism of early paleozoic geological complexes of Mongolia, Izvestiya-Physics of the Solid Earth, 53(3), 410-428.

Kovalenko, D. V., and V. A. Petrov (2017), Paleomagnetism of Mongolia, Doklady Earth Sciences, 472(1), 31-35.

Li, B. S., M. D. Yan, W. L. Zhang, X. M. Fang, Q. Q. Meng, J. B. Zan, Y. Chen, D. W. Zhang, Y. P. Yang, and C. Guan (2017), New paleomagnetic constraints on middle Miocene strike-slip faulting along the middle Altyn Tagh Fault, Journal of Geophysical Research-Solid Earth, 122(6), 4106-4122.

Li, S. H., E. L. Advokaat, D. J. J. van Hinsbergen, M. Koymans, C. L. Deng, and R. X. Zhu (2017), Paleomagnetic constraints on the Mesozoic-Cenozoic paleolatitudinal and rotational history of Indochina and South China: Review and updated kinematic reconstruction, Earth-Science Reviews, 171, 58-77.

Li, Z. Y., L. Ding, P. P. Song, J. J. Fu, and Y. H. Yue (2017), Paleomagnetic constraints on the paleolatitude of the Lhasa block during the Early Cretaceous: Implications for the onset of India-Asia collision and latitudinal shortening estimates across Tibet and stable Asia, Gondwana Research, 41, 352-372.

Lubnina, N. V., S. A. Pisarevsky, A. V. Stepanova, S. V. Bogdanova, and S. J. Sokolov (2017), Fennoscandia before Nuna/Columbia: Paleomagnetism of 1.98-1.96 Ga mafic rocks of the Karelian craton and paleogeographic implications, Precambrian Research, 292, 1-12.

Lund, S., L. Benson, R. Negrini, J. Liddicoat, and S. Mensing (2017), A full-vector paleomagnetic secular variation record (PSV) from Pyramid Lake (Nevada) from 47-17 ka: Evidence for the successive Mono Lake and Laschamp Excursions, Earth and Planetary Science Letters, 458, 120-129.

Lyu, P. L., W. X. Li, X. C. Wang, C. J. Pang, J. X. Cheng, and X. H. Li (2017), Initial breakup of supercontinent Rodinia as recorded by ca 860-840 Ma bimodal volcanism along the southeastern margin of the Yangtze Block, South China, Precambrian Research, 296, 148-167.

Mahgoub, A. N., H. Bohnel, C. Siebe, and M. O. Chevrel (2017), Paleomagnetic study of El Metate shield volcano (Michoacan, Mexico) confirms its monogenetic nature and young age (similar to 1250 CE), Journal of Volcanology and Geothermal Research, 336, 209-218.

Malandri, C., K. Soukis, M. Maffione, M. Ozkaptan, E. Vassilakis, S. Lozios, and D. J. J. van Hinsbergen (2017), Vertical-axis rotations accommodated along the Mid-Cycladic lineament on Paros Island in the extensional heart of the Aegean orocline (Greece), Lithosphere, 9(1), 78-99.

Marton, E., D. Zampieri, V. Cosovic, A. Moro, and K. Drobne (2017), Apparent polar polar wander path for Adria extended by new Jurassic paleomagnetic results from its stable core: Tectonic implications, Tectonophysics, 700, 1-18.

Lund, S., M. Schwartz, and L. Stott (2017), Long-term palaeomagnetic secular variation and excursions from the western Equatorial Pacific Ocean (MIS2-4), Geophysical Journal International, 209(2), 587-596.

Maffione, M., D. J. J. van Hinsbergen, G. de Gelder, F. C. van der Goes, and A. Morris (2017), Kinematics of Late Cretaceous subduction initiation in the Neo-Tethys Ocean reconstructed from ophiolites of Turkey, Cyprus, and Syria, Journal of Geophysical Research-Solid Earth, 122(5), 3953-3976.

Marko, F., P. A. M. Andriessen, C. Tomek, V. Bezak, L. Fojtikova, M. Bosansky, M. Piovarci, and P. Reichwalder (2017), Carpathian Shear Corridor - A strike-slip boundary of an extruded crustal segment, Tectonophysics, 703, 119-134.

Mattei, M., F. Cifelli, H. Alimohammadian, H. Rashid, A. Winkler, and L. Sagnotti (2017), Oroclinal bending in the Alborz Mountains (Northern Iran): New constraints on the age of South Caspian subduction and extrusion tectonics, Gondwana Research, 42, 13-28.

Meng, J., R. S. Coe, C. S. Wang, S. A. Gilder, X. X. Zhao, H. Liu, Y. L. Li, P. F. Ma, K. Shi, and S. Li (2017), Reduced convergence within the Tibetan Plateau by 26 Ma?, Geophysical Research Letters, 44(13), 6624-6632.

Michalski, K., G. Manby, K. Nejbert, J. Domanska-Siuda, and M. Burzynski (2017), Using palaeomagnetic and isotopic data to investigate late to post-Caledonian tectonothermal processes within the Western Terrane of Svalbard, Journal of the Geological Society, 174(3), 572-590.

Otofuji, Y., et al. (2017), Tectonic evolution of the Malay Peninsula inferred from Jurassic to Cretaceous paleomagnetic results, Journal of Asian Earth Sciences, 134, 130-149.

Pak, S. J., J. W. Moon, J. Kim, M. T. Chandler, H. S. Kim, J. Son, S. K. Son, S. K. Choi, and E. T. Baker (2017), Widespread tectonic extension at the Central Indian Ridge between 8 degrees S and 18 degrees S, Gondwana Research, 45, 163-179.

Pastor-Galan, D., K. F. Mulchrone, M. R. Koymans, D. J. J. van Hinsbergen, and C. G. Langereis (2017), Bootstrapped total least squares orocline test: A robust method to quantify vertical-axis rotation patterns in orogens, with examples from the Cantabrian and Aegean oroclines, Lithosphere, 9(3), 499-511.

Ponte, J. M., E. Font, C. Veiga-Pires, C. Hillaire-Marcel, and B. Ghaleb (2017), The effect of speleothem surface slope on the remanent magnetic inclination, Journal of Geophysical Research-Solid Earth, 122(6), 4143-4156.

Prezzi, C., C. Risso, M. J. Orgeira, F. Nullo, M. E. Sigismondi, and L. Margonari (2017), Subsurface architecture of Las Bombas volcano circular structure (Southern Mendoza, Argentina) from geophysical studies, Journal of South American Earth Sciences, 77, 247-260.

Ramos, V. A., C. Cingolani, F. Chemale, M. Naipauer, and A. Rapalini (2017), The Malvinas (Falkland) Islands revisited:

The tectonic evolution of southern Gondwana based on U-Pb and Lu-Hf detrital zircon isotopes in the Paleozoic cover, Journal of South American Earth Sciences, 76, 320-345.

Ran, B., B. Deng, C. S. Wang, X. X. Zhao, Y. L. Li, Y. X. Zhang, J. Meng, M. He, L. D. Zhu, and C. Xiao (2017), Kinematics of the crust around the Tanggula Shan in North-Central Tibet: Constraints from paleomagnetic data, Gondwana Research, 48, 124-133.

Rapalini, A. E., E. Tohver, L. S. Bettucci, A. C. Lossada, H. Barcelona, and C. Perez (2017), The late Neoproterozoic Sierra de las Animas Magmatic Complex and Playa Hermosa Formation, southern Uruguay, revisited: Paleogeographic implications of new paleomagnetic and precise geochronologic data (vol 259, pg 143, 2015), Precambrian Research, 295, 229-229.

Robert, B., J. Besse, O. Blein, M. Greff-Lefftz, T. Baudin, F. Lopes, S. Meslouh, and M. Belbadaoui (2017), Constraints on the Ediacaran inertial interchange true polar wander hypothesis: A new paleomagnetic study in Morocco (West African Craton), Precambrian Research, 295, 90-116.

Rodriguez-Parra, L., C. Gaitan, C. Montes, G. Bayona, and A. Rapalini (2017), Arc-seamount collision: driver for vertical-axis rotations in Azuero, Panama, Studia Geophysica Et Geodaetica, 61(2), 199-218.

Scandolara, J. E., R. T. Correa, R. A. Fuck, V. S. Souza, J. B. Rodrigues, P. S. E. Ribeiro, A. A. S. Frasca, A. M. Saboia, and J. V. Lacerda (2017), Paleo-Mesoproterozoic arc-accretion along the southwestern margin of the Amazonian craton: The Juruena accretionary orogen and possible implications for Columbia supercontinent, Journal of South American Earth Sciences, 73, 223-247.

Schmidt, P. W., and G. E. Williams (2017), Paleomagnetic age of ferruginous weathering beneath the Hamersley Surface, Pilbara, Western Australia, and the Cenozoic apparent polar wander path, Australian Journal of Earth Sciences, 64(2), 239-249.

Symons, D. T. A., K. Kawasaki, P. J. A. McCausland, and C. J. R. Hart (2017), Palaeopole for the 69 Ma Prospector Mountain stock: a critique of the Carmacks/'Baja BC' transport estimate for Yukon, Canada, Geophysical Journal International, 208(1), 349-367.

Tong, Y. B., Z. Y. Yang, J. L. Pei, H. Wang, Y. C. Xu, and Z. W. Pu (2017), Paleomagnetism of the Upper Cretaceous red-beds from the eastern edge of the Lhasa Terrane: New constraints on the onset of the India-Eurasia collision and latitudinal crustal shortening in southern Eurasia, Gondwana Research, 48, 86-100.

Uno, K., K. Furukawa, and Y. Hatanaka (2017), An analysis of apparent polar wander path for southwest Japan suggests no relative movement with respect to Eurasia during the Cretaceous, Physics of the Earth and Planetary Interiors, 267, 19-30.

Usui, Y., and W. Tian (2017), Paleomagnetic directional groups and paleointensity from the flood basalt in the Tarim large igneous province: implications for eruption frequency, Earth Planets and Space, 69.

Uzel, B., O. Sumer, M. Ozkaptan, C. Ozkaymak, K. Kuiper, H. Sozbilir, N. Kaymakci, U. Inci, and C. G. Langereis (2017), Palaeomagnetic and geochronological evidence for a major middle Miocene unconformity in Soke Basin (western Anatolia) and its tectonic implications for the Aegean region, Journal of the Geological Society, 174(4), 721-740.

Walczak, M. H., J. S. Stoner, A. C. Mix, J. Jaeger, G. P. Rosen, J. E. T. Channell, D. Heslop, and C. Xuan (2017), A 17,000 yr paleomagnetic secular variation record from the southeast Alaskan margin: Regional and global correlations, Earth and Planetary Science Letters, 473, 177-189.

Wen, B., D. A. D. Evans, and Y. X. Li (2017), Neoproterozoic paleogeography of the Tarim Block: An extended or alternative "missing-link" model for Rodinia?, Earth and Planetary Science Letters, 458, 92-106.

Wilkinson, J. J., K. Vowles, A. R. Muxworthy, and C. Mac Niocaill (2017), Regional remagnetization of Irish Carboniferous carbonates dates Variscan orogenesis, not Zn-Pb mineralization, Geology, 45(8), 747-750.

Wu, L., V. A. Kravchinsky, and D. K. Potter (2017), Apparent polar wander paths of the major Chinese blocks since the Late Paleozoic: Toward restoring the amalgamation history of east Eurasia, Earth-Science Reviews, 171, 492-519.

Xiong, J. G., Y. L. Li, Y. Z. Zhong, S. P. Si, J. H. Lei, W. L. Xin, X. Hu, and Y. F. Yao (2017), Paleomagnetic age of the Tangxian planation surface, northwestern Zhongtiao Shan of the Shanxi Graben System, North China, Geomorphology, 283, 17-31.

Yan, Y. G., B. C. Huang, J. Zhao, D. H. Zhang, X. H. Liu, P. Charusiri, and A. Veeravinantanakul (2017), Large southward motion and clockwise rotation of Indochina throughout the Mesozoic: Paleomagnetic and detrital zircon U-Pb geochronological constraints, Earth and Planetary Science Letters, 459, 264-278.

Zhao, L. M., A. Takasu, Y. J. Liu, and W. M. Li (2017), Blueschist from the Toudaoqiao Area, Inner Mongolia, NE China: Evidence for the Suture between the Ergun and the Xing'an Blocks, Journal of Earth Science, 28(2), 241-248.

Stratigraphy

Ai, K. K., J. L. Ji, G. C. Wang, K. X. Zhang, and Z. H. Tang (2017), Late Cenozoic magnetostratigraphy and anisotropy of magnetic susceptibility of the Baiyanghe section from the Hoxtolgay Basin: Implications for the uplift of the West Junggar Mt Range, NW China, Journal of Asian Earth Sciences, 138, 246-257.

Capraro, L., P. Ferretti, P. Macri, D. Scarponi, F. Tateo, E. Fornaciari, G. Bellini, and G. Dalan (2017), The Valle di Manche section (Calabria, Southern Italy): A high resolution record of the Early-Middle Pleistocene transition (MIS 21-MIS 19) in the Central Mediterranean, Quaternary Science Reviews, 165, 31-48.

Channell, J. E. T. (2017), Cobb Mountain Subchron recorded at IODP Site U1306 (Eirik Drift, off SE Greenland), Geophysical Journal International, 209(3), 1389-1397.

Channell, J. E. T. (2017), Complexity in Matuyama-Brunhes polarity transitions from North Atlantic IODP/ODP deep-sea sites, Earth and Planetary Science Letters, 467, 43-56.

Channell, J. E. T. (2017), Mid-Brunhes magnetic excursions in marine isotope stages 9, 13, 14, and 15 (286, 495, 540, and 590 ka) at North Atlantic IODP Sites U1302/3, U1305, and U1306, Geochemistry Geophysics Geosystems, 18(2), 473-487.

Channell, J. E. T. (2017), Magnetic excursions in the late Matuyama Chron (Olduvai to Matuyama-Brunhes boundary) from North Atlantic IODP sites, Journal of Geophysical Research-Solid Earth, 122(2), 773-789.

Channell, J. E. T., N. V. Riveiros, J. Gottschalk, C. Waelbroeck, and L. C. Skinner (2017), Age and duration of Laschamp and Iceland Basin geomagnetic excursions in the South Atlantic Ocean, Quaternary Science Reviews, 167, 1-13.

Chen, W. W., S. H. Zhang, J. K. Ding, J. H. Zhang, X. X. Zhao, L. D. Zhu, W. G. Yang, T. S. Yang, H. Y. Li, and H. C. Wu (2017), Combined paleomagnetic and geochronological study on Cretaceous strata of the Qiangtang terrane, central Tibet, Gondwana Research, 41, 373-389.

Gong, Z., K. P. Kodama, and Y. X. Li (2017), Rock magnetic cyclostratigraphy of the Doushantuo Formation, South China and its implications for the duration of the Shuram carbon isotope excursion, Precambrian Research, 289, 62-74.

Guzhikov, A. Y., E. Y. Baraboshkin, V. N. Beniamovsky, V. S. Vishnevskaya, L. F. Kopaevich, E. M. Pervushov, and A. A. Guzhikova (2017), New Bio- and Magnetostratigraphic Data on Campanian-Maastrichtian Deposits of the Classical Nizhnyaya Bannovka Section (Volga River Right Bank, Southern Saratov Region), Stratigraphy and Geological Correlation, 25(1), 39-75.

Hagstrum, J. T., R. J. Fleck, R. C. Evarts, and A. T. Calvert (2017), Paleomagnetism and Ar-40/Ar-39 geochronology of the Plio-Pleistocene Boring Volcanic Field: Implications for the geomagnetic polarity time scale and paleosecular variation, Physics of the Earth and Planetary Interiors, 262, 101-115.

Hounslow, M. W., G. McIntosh, R. A. Edwards, D. J. C. Laming, and V. Karloukovski (2017), End of the Kiaman Superchron in the Permian of SW England: magnetostratigraphy of the Aylesbeare Mudstone and Exeter groups, Journal of the Geological Society, 174(1), 56-74.

Irace, A., G. Monegato, E. Tema, E. Martinetto, D. Gianolla, E. Vassio, L. Bellino, and D. Violanti (2017), Unconformity-bounded stratigraphy in the Plio-Pleistocene continental record: new insights from the Alessandria Basin (NW Italy), Geological Journal, 52(2), 177-206.

Ji, J. L., K. X. Zhang, P. D. Clift, G. S. Zhuang, B. W. Song, X. Ke, and Y. D. Xu (2017), High-resolution magnetostratigraphic study of the Paleogene-Neogene strata in the Northern Qaidam Basin: Implications for the growth of the Northeastern Tibetan Plateau, Gondwana Research, 46, 141-155.

Kent, D. V., P. E. Olsen, and G. Muttoni (2017), Astrochronostratigraphic polarity time scale (APTS) for the Late Triassic and Early Jurassic from continental sediments and correlation with standard marine stages, Earth-Science Reviews, 166, 153-180.

Krause, J. M., W. C. Clyde, M. Ibanez-Mejia, M. D. Schmitz, T. Barnum, E. S. Bellosi, and P. Wilf (2017), New age constraints for early Paleogene strata of central Patagonia, Argentina: Implications for the timing of South American Land Mammal Ages, Geological Society of America Bulletin, 129(7-8), 886-903.

Kravchinsky, V. A. (2017), Magnetostratigraphy of the Lake Baikal sediments: A unique record of 8.4 Ma of continuous sedimentation in the continental environment, Global and Planetary Change, 152, 209-226.

Kuzmina, O. B., Z. N. Gnibidenko, L. B. Khazin, and I. V. Khazina (2017), New data on stratigraphy (palynomorphs, ostracods, paleomagnetism) of Cenozoic continental deposits of the Ishim plain, Western Siberia, Stratigraphy and Geological Correlation, 25(3), 342-361.

Li, B. F., D. H. Sun, W. H. Xu, F. Wang, B. Q. Liang, Z. W. Ma, X. Wang, Z. J. Li, and F. H. Chen (2017), Paleomagnetic chronology and paleoenvironmental records from drill cores from the Hetao Basin and their implications for the formation of the Hobq Desert and the Yellow River, Quaternary Science Reviews, 156, 69-89.

Llanos, M. P. I., D. A. Kietzmann, M. K. Martinez, and R. M. Palma (2017), Magnetostratigraphy of the Upper Jurassic-Lower Cretaceous from Argentina: Implications for the J-K boundary in the Neuquen Basin, Cretaceous Research, 70, 189-208.

Luberti, G. M., F. Marra, and F. Florindo (2017), A review of the stratigraphy of Rome (Italy) according to geochronologically and paleomagnetically constrained aggradational successions, glacio-eustatic forcing and volcano-tectonic processes, Quaternary International, 438, 40-67.

Maron, M., G. Muttoni, M. J. Dekkers, M. Mazza, G. Roghi, A. Breda, W. Krijgsman, and M. Rigo (2017), Contribution to the magnetostratigraphy of the Carnian: new magneto-biostratigraphic constraints from Pignola-2 and Dibona marine sections, Italy, Newsletters on Stratigraphy, 50(2), 187-203.

Mayr, C., et al. (2017), Nesseltalgraben, a new reference section of the last glacial period in southern Germany, Journal of Paleolimnology, 58(2), 213-229.

Milanese, F. N., E. B. Olivero, J. L. Kirschvink, and A. E. Rapalini (2017), Magnetostratigraphy of the Rabot Formation, Upper Cretaceous, James Ross Basin, Antarctic Peninsula, Cretaceous Research, 72, 172-187.

Minguez, D., and K. P. Kodama (2017), Rock magnetic chronostratigraphy of the Shuram carbon isotope excursion: Wonoka Formation, Australia, Geology, 45(6), 567-570.

Noguchi, A., H. Oda, Y. Yamamoto, A. Usui, M. Sato, and J. Kawai (2017), Scanning SQUID microscopy of a ferromanganese crust from the northwestern Pacific: Submillimeter scale magnetostratigraphy as a new tool for age determination and mapping of environmental magnetic parameters, Geophysical Research Letters, 44(11), 5360-5367.

Ojala, A. E. K., T. P. Luoto, and J. J. Virtasalo (2017), Establishing a high-resolution surface sediment chronology with multiple dating methods - Testing Cs-137 determination with Nurmijarvi clastic-biogenic varves, Quaternary Geochronology, 37, 32-41.

Rovey, C. W., G. Balco, M. Forir, and W. F. Kean (2017), Stratigraphy, paleomagnetism, and cosmogenic-isotope burial ages of fossil-bearing strata within Riverbluff Cave, Greene County, Missouri, Quaternary Research, 87(3), 516-528.

Scholze, F., X. Wang, U. Kirscher, J. Kraft, J. W. Schneider, A. E. Goetz, M. M. Joachimski, and V. Bachtadse (2017), A multistratigraphic approach to pinpoint the Permian-Triassic boundary in continental deposits: The Zechstein-Lower Buntsandstein transition in Germany, Global and Planetary Change, 152, 129-151.

Simon, Q., et al. (2017), Authigenic Be-10/Be-9 ratio signature of the Matuyama-Brunhes boundary in the Montalbano Jonico marine succession, Earth and Planetary Science Letters, 460, 255-267.

Suteerasak, T., S. A. Elming, G. Possnert, J. Ingri, and A. Widerlund (2017), Deposition rates and C-14 apparent ages of Holocene sediments in the Bothnian Bay of the Gulf of Bothnia using paleomagnetic dating as a reference, Marine Geology, 383, 1-13.

Weiner, T., J. Kalvoda, T. Kumpan, E. Schindler, and D. Simicek (2017), An Integrated Stratigraphy of the Frasnian-Famennian Boundary Interval (Late Devonian) in the Moravian Karst (Czech Republic) and Kellerwald (Germany), Bulletin of Geosciences, 92(2), 257-281.

Other

Arato, R., and A. Audetat (2017), Experimental calibration of a new oxybarometer for silicic magmas based on vanadium partitioning between magnetite and silicate melt, Geochimica Et Cosmochimica Acta, 209, 284-295.

Arato, R., and A. Audetat (2017), Vanadium magnetite-melt oxybarometry of natural, silicic magmas: a comparison of various oxybarometers and thermometers, Contributions to Mineralogy and Petrology, 172(7).

Wang, D. Y., D. Y. Han, W. Q. Li, Z. P. Zheng, and Y. C. Song (2017), Magnetic-resonance imaging and simplified Kozeny-Carman-model analysis of glass-bead packs as a frame of reference to study permeability of reservoir rocks, Hydrogeology Journal, 25(5), 1465-1476.

cont'd. from pg. 1...

Fig. 2. Sample preparation area.

John T Tate Laboratory of (Geo)Physics.

The location.

As disclosed in the IRM Quarterly v25-2, the IRM has moved to the second floor of the newly renovated Tate Hall, on the University of Minnesota Mall. The previous building plan was U shaped*, and the exterior "shell" of this structure was preserved, while the interior spaces were completely gutted and redesigned, for offices and labs. The center of the building was filled by a new addition, which hosts the larger lecture theaters on the ground and basement levels, smaller classrooms/meeting rooms, and graduate student offices on the "higher" levels. A spacious naturally lit atrium and side corridors separate the old building from the new addition, which also means that all labs and offices (other than the few in the sub-basement…) have natural light shining through HUGE windows (often looking onto other offices…). For a map location of Tate Hall please visit our website, http://www.irm.umn.edu/IRM/location.html

The works.

Probably the biggest change within the new set-up is brought about by the open floor plan that we chose for the IRM (fig. 1). The main lab space is located in room 240, in the southern wing of Tate Hall. Walking through the lab main entrance one finds the sample prep area, with fume hood, sinks, balance and supplies directly to the left (fig. 2). To the right is the "susceptibility corridor", which lines the outer wall of the shielded room, with KLY, MFK and Magnon available to measure low-field susceptibility and its dependence on temperature, orientation, frequency and AC field strength (fig. 3). At the end of the corridor, room (240-02) houses the compressors for the 2Gs and our rock saws and polishers, our "dirty prep" lab in a nutshell, literally.

Fig. 3. The "susceptibility corridor"

The brand new feature of the lab is, of course, the new shielded room, located in the southwest corner. The new room is somewhat narrower but longer than the old one (11 by 22.5 feet), for a total area a few square feet larger. The arrangement has the old 2G (RF SQUIDs) on the south and U-Channel along the north wall, with the furnaces stacked up in between (fig. 4). This leaves ample space towards the entrance for the D-Tech (de) magnetizer and sample storage and maybe a new SQUID microscope, if proposal reviews and NSF budget constraints are sufficiently favorable.

In front of the shielded room entrance are a "meeting" area and mobile workstations which host/define the imaging area of the lab, notably the MFM and other microscopes.

On the opposite side of the lab is the high-field area, technically room 244-01. Here the MPMSs and the VSMs are located (fig. 5). The MPMSs are right in front of a sound proof room, which hosts the noisy helium liquefier system, hopefully making the MPMS experience

Fig. 4. The shielded room.

a more pleasant one altogether. Likewise, the AGM now has a dedicated sound-proof room of its own in the in southeast corner.

The Mössbauer lab is enclosed in its own secure space located next door to the helium liquefier room and will feature our brand new Mössbauer spectrometer (for a grand total of three spectrometers), awaiting its first ever specimen. Last but not least, Peat Solheid's office is situated within the lab space, in the far northeast corner. The rest of the IRM faculty/staff and post-doc offices are opposite the lab, including the Visiting Fellow office that is shared with the founding father, Subir Banerjee.

That sums up a "tour" of the new lab, so I leave you with a reminder of the new mailing address for the IRM:

IRM, Department of Earth Sciences,
150 John T Tate Hall,
116 Church St. SE,
Minneapolis, MN 55455.

Phone numbers remain unchanged, and if you are visiting the lab, come straight up to the second floor: #240 marks the spot. We look forward to seeing you there!

*The original 1930s building consisted of the west wing, facing Northrop mall; the north and south wings were added in the 1960s.

The Next
Visiting Fellow
Application Deadline
is

October 31st

Visit our website for details and application information:

www.irm.umn.edu


Fig. 5. The magnetic imaging area.


Fig. 6. The high field area.

University of Minnesota
291 Shepherd Laboratories
100 Union Street S. E.
Minneapolis, MN 55455-0128
phone: (612) 624-5274
fax: (612) 625-7502
e-mail: irm@umn.edu
www.irm.umn.edu

The IRM Quarterly

The *Institute for Rock Magnetism* is dedicated to providing state-of-the-art facilities and technical expertise free of charge to any interested researcher who applies and is accepted as a Visiting Fellow. Short proposals are accepted semi-annually in spring and fall for work to be done in a 10-day period during the following half year. Shorter, less formal visits are arranged on an individual basis through the Facilities Manager.

The *IRM* staff consists of **Subir Banerjee**, Professor/Founding Director; **Bruce Moskowitz**, Professor/Director; **Joshua Feinberg**, Assistant Professor/Associate Director; **Mike Jackson, Peat Sølheid** and **Dario Bilardello**, Staff Scientists.

Funding for the *IRM* is provided by the **National Science Foundation**, the **W. M. Keck Foundation**, and the **University of Minnesota**.

The *IRM Quarterly* is published four times a year by the staff of the *IRM*. If you or someone you know would like to be on our mailing list, if you have something you would like to contribute (*e.g.*, titles plus abstracts of papers in press), or if you have any suggestions to improve the newsletter, please notify the editor:

Dario Bilardello
Institute for Rock Magnetism
Department of Earth Sciences
University of Minnesota
150 John T Tate Hall
116 Church Street SE
Minneapolis, MN 55455-0128
phone: (612) 624-5274
e-mail: dario@umn.edu
www.irm.umn.edu

UNIVERSITY OF MINNESOTA